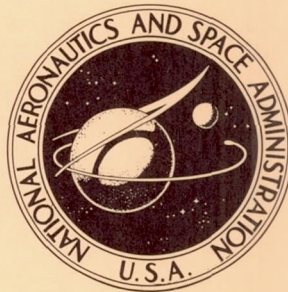


NASA TECHNICAL NOTE



NASA TN D-5055

NASA TN D-5055

A METHOD FOR CHARACTERIZING
THE SURFACE CLEANLINESS
DURING ADHESION TESTING

by James M. Bradford, Jr.

Langley Research Center

Langley Station, Hampton, Va.

A METHOD FOR CHARACTERIZING THE SURFACE CLEANLINESS
DURING ADHESION TESTING

By James M. Bradford, Jr.

Langley Research Center
Langley Station, Hampton, Va.

NATIONAL AERONAUTICS AND SPACE ADMINISTRATION

For sale by the Clearinghouse for Federal Scientific and Technical Information
Springfield, Virginia 22151 - CFSTI price \$3.00

A METHOD FOR CHARACTERIZING THE SURFACE CLEANLINESS DURING ADHESION TESTING

By James M. Bradford, Jr.
Langley Research Center

SUMMARY

It has been shown that the degree of adhesion of metals depends upon the surface cleanliness. This paper presents a method that was used to characterize the surface cleanliness of nickel during an adhesion experiment. The change in the work function of the surface as the metal was cleaned was used to indicate the degree of cleanliness. The point at which the work function was stable with additional cleaning was used as the cleanest surface. The cleaning technique was an argon-ion bombardment and heating process. Measurements of the adhesion force showed that the maximum adhesion forces occurred when the surfaces were the cleanest. The cleaned surfaces were recontaminated with oxygen and the adhesion force decreased to zero.

INTRODUCTION

Recently, there has been an enlarged interest in the field of the adhesion of metallic surfaces. Some of this interest is undoubtedly due to the problems involved when metals are used in the low-pressure environment of outer space. The greatest impetus, however, to the study of the adhesion of metal surfaces and, indeed to surfaces themselves, has been given by the recent availability of the equipment and techniques to allow the investigation of surfaces. Only within the last decade has vacuum technology advanced to the stage that pressures can be attained low enough to allow the study of uncontaminated surfaces. The invention and development of such devices as the low-energy electron-diffraction device (LEED) and the field ion microscope have also come only recently. These instruments allow individual atoms or groups of atoms at the surface to be studied.

Metal-to-metal adhesion is a potential problem in the space environment. Since most conventional lubricants fail under the conditions found in space, problems arise with the seizure of bearings and other moving parts. Other potential problems arise in the adhesion of metal parts under normal contact loads such as relay contacts or valve seats. In the past, each potential problem of metallic adhesion was treated on an individual basis and the solution applied only to a limited class of adhesion problems.

A general study of the adhesion phenomena on a more fundamental basis would allow general solutions to adhesion problems to be formulated.

It is important to know the degree of contamination of the surface to be studied because in an adhesion test it has been shown (refs. 1 and 2) that the existence of one or two monolayers of contaminants at the surface can prevent or reduce the amount of adhesion. Thus, the degree of contamination of the surface must be determined by some method that would detect the presence of a fraction of a monolayer. Even though many workers (refs. 1, 3, and 4) have reported various methods for preparing surfaces for adhesion testing, few of these report on any technique used to determine the degree of contamination of the surface. Unless such a technique is used to show that the surface is clean before it is joined, there is no way to determine how much of the contact force used to form the adhesion junction is required to disrupt the contaminant film.

The purpose of this paper is to present the development of a method for characterizing the surface cleanliness of nickel surfaces during adhesion testing and to show the relationship between the degree of surface cleanliness and the adhesion coefficient. The variation of the adhesion coefficient for cleaned nickel surfaces as a function of the degree of oxygen recontamination is also presented and a discussion of the theory of adhesion is included as appendix A.

SYMBOLS

C	constant
e	electronic charge, coulombs
F	flux of molecules striking sample surface, molecules/centimeter ² /second
F _i	flux of molecules striking sample surface for ith gas, molecules/centimeter ² /second
F _b	breaking force, newtons
I	electron current to anode, amperes
I ₊	argon ion current, amperes
k	Boltzmann constant

m_i	mass of molecule of ith gas, grams
M_i	molecular weight of ith gas
p	pressure, torr
p_i	partial pressure of ith gas, torr
R	resistance of source of current for diode, ohms
S	sputtering rate, molecules of nickel removed per incident argon ion
T	cathode temperature, $^{\circ}\text{K}$
T_i	temperature of ith gas, $^{\circ}\text{K}$
V_A	anode-cathode voltage, volts
V_B	electromotive force generated by battery, volts
W_{AB}	work of adhesion between bulk phases A and B
Y	sputtering yield in atoms
α	adhesion coefficient, ratio of adhesion force divided by contact force
γ_{ij}	interfacial energy (i_0 is solid-vacuum interface and ij is solid-solid interface)
ζ	ratio of nickel atoms sputtered to maximum contamination rate
θ	fraction of σ_m that is filled
μ	dipole moment per adsorbed site
σ_m	adsorption sites per centimeter ²

ϕ	work function, electron volts
χ	surface potential, volts

EXPERIMENTAL APPROACH

Surface Cleaning Technique

The procedure used in this investigation to clean the surfaces of the samples is one proposed and used by Farnsworth (ref. 5). It consists of cycles of inert-gas ion bombardment and heating. This cleaning procedure has been used to study the surface of titanium, germanium (ref. 6), silicon, nickel (ref. 5), and tantalum (ref. 7).

Many other workers have used the technique to clean metals. Mac Rae (ref. 8), for instance, has conducted a study of the surface of clean nickel crystals using the ion bombardment and heating method of cleaning.

Farnsworth (ref. 5) discussed the way in which the cleaning procedure affects the nickel surface. After outgassing the sample for several hours at 800° C, the surface was covered with an impurity (probably carbon) which diffused to the surface during the heating process. The subsequent ion bombardment removed the carbon, but the relatively high carbon density just below the surface resulted in the recontamination of the surface when the sample was heated. The clean surface could only be created and maintained after the cleaning cycle had been repeated enough times until the carbon density was too low to recontaminate the surface during the heat treatment.

In the investigations of the clean surfaces using the LEED device, the experiment itself produced evidence of the degree of cleanliness of the surfaces. Since this investigation was not conducted with single crystals, it was not possible to use the LEED device, and some other measure of the cleanliness of the surface had to be used. This measure was the change in the work function of the surface.

Change of Work Function With Surface Contamination

There have been numerous observations of the change in the work function of a surface with the degree of contamination of the surface. Excellent summaries on this topic are given in references 9 and 10. The effect of the contamination on the surface is most easily described (ref. 9) by considering the contaminating molecules to form a dipole layer at the surface which alters the surface potential χ . The resulting change in the work function of the surface is then given by

$$\Delta\phi = 4\pi\sigma_m\theta\mu \quad (1)$$

where θ is the filled fraction of the total number of adsorption sites per cm^2 (σ_m) and μ is the dipole moment per adsorbed site. This analysis is valid only for low values of θ and takes into account only one of the parameters which can cause the work function to change. Such parameters as the heterogeneous nature of the surface which arises from different crystal faces, lattice defects, dislocations, and so forth, can also affect the work function. The effect of contamination on the surface is, however, the larger effect (ref. 9), and the work function of the surface is a strong function of the degree and kind of contamination present on the surface. It has been observed (ref. 11) for certain systems that the presence of 1/100 of a monolayer alters the work function of a surface so that it is possible that the change in the work function can indicate very small amounts of surface contamination. The equation relating the change in work function with the change of contamination is very simplified and, at best, can predict the correct results for low values of θ . It appears that the work function can then be used to characterize the degree of contamination only in a qualitative way, especially for highly contaminated surfaces.

Eisinger has measured the change in the work function of tungsten with the adsorption of nitrogen (ref. 12) and carbon monoxide (ref. 13). In both cases the work function was an approximately linear function of the number of atoms adsorbed on the surface at least up to a single monolayer coverage. Redhead (ref. 14) has also measured the change in work function of tungsten with the adsorption of nitrogen and carbon monoxide, and although the results are somewhat different than those reported by Eisinger (ref. 13), there is still a linear relationship between the change in work function and the number of atoms adsorbed for low values of monolayer coverage. Theoretical discussions of the change in work function on monolayer adsorption are given in references 9, 10, and 15.

DESCRIPTION OF APPARATUS

Vacuum System

The experiment was conducted at very low pressure so that the sample surfaces, once cleaned, would stay clean for a reasonable length of time. Therefore, the experimental apparatus was installed in a vacuum chamber. The vacuum chamber was a horizontal cylinder 30 inches (0.762 m) in diameter and 42 inches (1.02 m) long. The vacuum chamber and the apparatus attached to the vacuum chamber are shown in figure 1. The vacuum chamber was pumped by a 10-inch (0.254-m) oil diffusion pump which was backed by a 2-inch (0.051-m) diffusion pump and a mechanical roughing pump. A water-cooled baffle and a liquid nitrogen-cooled baffle were located between the diffusion pump and the chamber to prevent oil backstreaming. The pressure in the chamber after the chamber has been baked and with the experimental apparatus installed was

typically 5×10^{-10} torr (1 torr = 133.32 N/m²). Additional details of the vacuum system are given in reference 16.

Also shown in figure 1 are the electronic equipment in the relay racks to the right of the vacuum chamber and the loading frame and load-measuring equipment on the left of the vacuum chamber. More details about this equipment are given subsequently.

Apparatus For Measuring Work Function

The retarding field diode method (ref. 17) was chosen to measure the changes in the sample work function. The method is relatively simple and can give a continuous recording of the sample work function. Under certain conditions (see appendix B) the change in the sample work function is the same as the change in the sample voltage. The work function change is then measured by measuring the change in the sample voltage. The left sample was mounted on the end of a linear motion feedthrough and the right sample was mounted in a sample holder which was affixed to a rotary turntable. Water-cooled tubes were attached to the sample mounts in order to keep them cool during the heating cycle. The right sample could be rotated by using a rotary motion feedthrough shown in figure 1. The electrical schematic of the apparatus used to measure the work function is shown in figure 2. The apparatus used for measuring the change in the work function is shown in figure 3. This apparatus consisted of three main parts: the ion bombardment apparatus, the electron gun apparatus, and the rotation apparatus.

A closeup of the apparatus is seen in figure 4. The electron gun is shown behind the right sample holder. The samples were electrically insulated from the sample holders by alumina spacers. Also shown in figure 4 is the turntable lock. This device locked the turntable in place when the left sample was traversed inward. The position indicator allowed the turntable to be set at the exact position required. Also shown in figure 4 are the ion gun and the gas inlet tube which fed the argon into the back of the ion gun.

Magnetron Ion Gun

The magnetron ion gun apparatus was used during the cleaning procedure before the work function measurements were made. It consisted of a cold cathode ion source and its associated power supplies. A schematic of the magnetron ion gun is shown in figure 5. The ion source was a modified magnetron configuration (ref. 18), which used, in this case, an anode voltage of 2000 volts and an axial magnetic field of 600 gauss.

The gas was injected into the discharge space through the end of the back cathode. Ions were extracted from the opposite end of the discharge space through the front cathode. The front cathode was shaped to cause the electric field at that end of the discharge to extract ions from the discharge. The extracted ions were focused into a beam as they passed through the cylindrical lens system. Electrostatic deflection plates at the exit of

the focusing cylinder could deflect the ion beam slightly so that it could be positioned on a target. The gun was normally operated with the anode at 2000 volts and both the front and back cathode grounded. An extraction potential of -1300 volts was applied to grids 1 and 2 and to the focusing cylinder nearest the grids. The other focusing cylinder was grounded.

The ion current to a target 1 square centimeter in area was measured as a function of pressure. In the pressure range of 10^{-8} torr to 10^{-6} torr, the ion current-pressure relationship is given by

$$I_+ = 0.35p \quad (2)$$

where I_+ is the ion current in amperes on a target 1 centimeter square, and p is the pressure in the vacuum chamber in torrs.

The energy distribution in the ion beam was measured by placing a faraday cup behind a retarding grid and focusing the ion beam through the retarding grid into the faraday cup. For the normal operating conditions already stated, the maximum ion energy was found to be about 1300 electron volts. The distribution of ion current density over the width of the beam was measured by placing a glass plate with a hole in it in the ion beam. The hole in the plate was 1/8 inch (0.3 cm) in diameter and a collector plate covered the hole on the back of the plate. The plate was rotated across the beam and the ion current measured during the traverse across the beam. The results of the test showed that the current density varied ± 10 percent over a 2-centimeter beam width.

Electron Gun Used During Work Function Measurements

The electron gun apparatus used in making the work function measurements consisted of an electron gun and its associated power supplies. A schematic drawing of the electron gun is shown in figure 6. The cathode was made of tungsten ribbon. The attachment rods and support posts for the cathode were also made of tungsten so that the filament could be degassed at very high temperatures. The anode was made of nickel sheet and the aperture in the anode was 0.5 mm in diameter.

As shown in equation (6), the change in sample voltage is equal to the change in the work function only if the temperature of the cathode is held constant. This constant temperature was obtained by maintaining a constant voltage across the cathode with a programmable power supply. Figure 2 is an electrical schematic of the work function apparatus. The electromotive force V_B was provided by a 30-volt mercury battery and the resistance R is a 2×10^{10} -ohm resistor. The sample voltage V_A was measured by an electrometer with an input resistance greater than 10^{14} ohms and was recorded on a strip-chart recorder. In order to insure that the sample voltage V_A was in the retarding field region, the voltage-current relationship was measured while a retarding

voltage was being applied to the sample. The sample voltage was in the retarding field region if it was less than 1 volt. A test procedure to determine the drift and stability of the work function showed that the work function could be held constant to within ± 0.005 volt.

Rotation Apparatus

The rotation apparatus consisted of the samples and the apparatus necessary to put the samples into the positions to heat, to bombard with ions, and to measure the work function. Figure 7 shows a closeup view of the initial adhesion apparatus in the position used to bombard the samples with ions. In this position, the cam surfaces have raised the electron gun out of the way, and the samples are in a position so that they can be bombarded with ions by the ion gun. In this position, the samples could also be heated by the heating filament.

If the right sample were rotated 90° , as shown in figure 8, the work function of the right sample could be measured. In this position the cam surfaces had lowered the gun until it was opposite the face of the right target. This position was used for all the work function measurements.

It was originally planned to use the same apparatus for measuring the change in the work function and the adhesion coefficient. It was discovered during the course of the experimentation that nickel samples required much more ion dosage to clean the surfaces than did stainless steel or tungsten (ref. 18) upon which the initial estimates of the required ion current density had been made. Thus, the ion gun used during the work function measurements did not have enough ion current density to clean the samples in a reasonable length of time.

When the requirement for a higher ion current density was discovered, a new hot cathode ion gun was developed to give the higher ion current density. The physical arrangement of the hot cathode ion gun and the fact that its magnetic field extended into the region of the samples precluded the measurement of the change in the work function of the sample when the hot cathode ion gun was installed. The hot cathode ion gun was used for both the ion bombardment and the heating.

Adhesion Apparatus

The apparatus used during the adhesion tests is shown installed in the vacuum chamber in figure 9. The apparatus consisted of the hot cathode ion gun and the adhesion apparatus. The turntable was locked into position and did not rotate.

Samples

The samples were machined from very pure (99.997 percent) polycrystalline nickel rod. A set of the samples is shown in figure 10, along with the dimensions of the samples. The front faces of the samples were ground by using successive grit sizes of silicon carbide paper of 240, 320, 400, and 600. They were rough polished on nylon cloth by using successive pastes of 15- and 8-micrometer size followed by a 1-micrometer diamond paste on Beuhler microcloth. Final polishing was on Beuhler microcloth by using Beuhler gamma alumina micropolish of 0.05-micrometer size. After final polishing, the samples were cleaned in an ultrasonic cleaner by using successive solutions of a mild detergent, deionized water, acetone, and methanol.

Hot Cathode Ion Gun

A closeup of the hot cathode ion gun installed in the vacuum chamber is shown in figure 11. The permanent magnets provided an axial magnetic field of approximately 200 gauss. The reflector electrode reflected the electrons as they emerged from the electron gun and so increased the path length of the electrons in the vicinity of the samples. A schematic drawing of the hot cathode ion gun is shown in figure 12. The filament was 1-percent thoriaated tungsten wire, and the grid was made from 0.0005-inch-diameter tungsten wire with 120 wires to the inch. The other parts of the gun were made from 0.010-inch-thick nickel sheet.

The hot cathode ion gun was used in both the ion bombardment and the heating cycles. In the ion bombardment cycle, the filament was biased at -180 volts and the lens was grounded. Argon that had been purified was admitted into the back of the gun through the gas inlet tube shown in figure 12. The argon was ionized by the electrons being emitted from the filament, and the argon ions were then accelerated into the samples which were biased to -2000 volts. The total emission current from the filament was approximately 50 milliamperes.

The variation of ion current with pressure is shown in figure 13. It is seen that the output of the gun varied from 18 microamperes at a pressure of 2×10^{-7} torr to 360 microamperes at 3×10^{-5} torr. The variation of ion current with sample voltage is shown in figure 14. The ion current increased with sample voltage up to the highest voltage tested which was 2400 volts.

When being used for heating the samples, the potentials on the hot-cathode ion gun were the same as those for the ion bombardment but the potential on the samples was +1200 volts. The current to each of the samples during heating was about 10 milliamperes.

Gas Purification System

It was stated that the argon gas was purified previous to being admitted into the vacuum system. The argon was initially very pure (99.996 percent), but it was discovered that still further purification was necessary in order to get the pure argon into the vacuum system. This purification was accomplished by admitting the argon through an isolation valve into a previously baked evacuated titanium sublimation pump which was isolated from the vacuum chamber by a variable leak valve. (See fig. 15.) The argon was admitted into the evacuated sublimation pump until the pressure was about 1000 micrometers, and the sublimation pump was flashed and the impurities in the argon were gettered. The very pure argon was then admitted into the vacuum chamber through the variable leak valve.

Mass Spectrometer

The level of contamination in the argon was monitored during the ion-bombardment cycle by a cycloidal-type mass spectrometer mounted on the vacuum system as shown in figure 16. The instrument had a sensitivity of about 10^{-11} torr for nitrogen and unit resolution at about mass 75. It was necessary to use the mass spectrometer in the procedure because without it the level of impurities in the system could not have been known, and the rate of contamination of the sample surfaces during the ion bombardment and heating procedures could not have been calculated.

Load Cell

The load cell which was used to measure the force is shown installed in the chamber in figure 9 and in more detail in figure 17. It was calibrated with weights over the range that it was to be used before and after each set of samples was tested, and it remained accurate to within 1/2 pound (2.224 N). A separate load cell outside the chamber was used periodically to give an approximate check on the operation of the inside load cell. The output of the load cell was measured on a 0- to 1-mV full-scale recorder and could be attenuated in steps so that full-scale indications of 200 pounds (889.6 N), 400 pounds (1779.2 N), or 800 pounds (3558.4 N), could be recorded. The load cell was balanced, and the voltage was checked before each force measurement.

Pressure Measurement

The pressure was measured by a Veeco RG-75 gage tube and an RG-21 controller. The output of the controller was fed into a recorder so that the pressure could be recorded continuously during the experiment. A nude Varian gage was also mounted on the vacuum system, but since the two gages indicated approximately the same, the pressure from the Varian gage was not recorded continuously.

Temperature Measurement

A chromel-alumel thermocouple was attached to each specimen in order to measure the temperature during the annealing part of the cleaning cycle. The output of the thermocouples was measured by a potentiometer pyrometer.

Electrical Schematic

The electrical schematic for the experimental apparatus is shown in figure 18. The switches shown allowed the ion bombardment or heat cycles to be selected and also allowed the temperatures of each specimen to be measured during the heat cycle.

PROCEDURE

Procedure For Measuring Work Function

After the samples had been installed and aligned, the vacuum chamber was evacuated and baked for approximately 8 hours at 200° C. After the chamber had cooled, the electron gun (see fig. 6) was turned on and vigorously outgassed with the anode temperature high enough to cause it to turn a dull red color. After the gun was cooled to its normal operating temperature, the cathode temperature was adjusted so that the sample voltage V_A was approximately zero. This initial adjustment of the sample voltage at 0 volts allowed the voltmeter to be set on a scale sensitive enough to allow small changes in the sample voltage to be measured. After the correct cathode temperature had been determined, it was maintained by the programable power supply.

The samples were heated to approximately 550° C for 1 hour to outgas them initially, and after they had cooled to ambient temperature, the relative work function was measured. Depending upon the particular test sequence, the samples were then either ion bombarded or heated and the work function subsequently measured.

For the work function measurements, the magnetron ion gun was used to bombard the samples with ions. Since this type ion gun has no hot filament, the ion-bombardment procedure was to apply the operating voltages to the ion gun and then to let the argon into the gun. The ion current to each specimen was measured by a coulombmeter. This instrument indicated the magnitude of the ion current as well as integrating the current to give the total ion dosage for each sample. When the desired dosage had been attained on each sample, the argon was cut off and the ion-bombardment sequence ended.

Heating the specimens during the cleaning procedure prior to the work function measurements was accomplished by placing a potential of +1200 volts on the samples and then electron bombarding the samples by using the heating filament previously described. A temperature of approximately 1200° F (648.8° C) could be attained in about 2 minutes

by using this technique. The heating filament was located so that no tungsten could be evaporated from it and reach the front face of either sample.

Measurement of Adhesion Coefficient

The procedure for ion bombarding with the hot cathode ion gun (fig. 12) was as follows. The filament was turned on and the filament bias and sample voltage were applied. The argon was then admitted into the back of the gun and the bombardment of the samples initiated. Since the samples were at a voltage of -2000 volts, it was not feasible to use the coulombmeter to measure the dosage as with the initial apparatus; thus, the ion current was recorded every minute and later integrated to give the total dosage.

The heating of the samples with the adhesion apparatus was similar to heating during the cleaning procedure before the work function measurements except that the hot cathode ion gun was used as the source of electrons instead of the heating filament.

The force was applied to the samples by a push-pull mechanism which was attached to a screw jack which was, in turn, actuated by a variable-speed motor. The speed of the motor was controllable so that displacement rates from about 1.8×10^{-3} inch per minute to 0.4 inch per minute could be used. To make an adhesion test, the samples were first allowed to cool to about 350° F (176.6° C) and then were pressed together by traversing the left sample inward until the predetermined load was indicated on the load cell. The load was measured continuously and recorded on the strip-chart recorder. A typical adhesion test sequence as recorded is shown in figure 19. The load was applied while the load cell was indicating compressive loads. After the desired load was attained, the left sample was stopped from traversing inward and the load decreased slightly because of creep. After a predetermined time, the load was removed by traversing the left sample outward. When the load cell indicated zero load, the polarity of the output of the load cell was changed so that the load cell was then indicating tension. The left sample continued to traverse outward at a constant rate of 1.8×10^{-3} inch ($4.57 \mu\text{m}$) per minute until the samples broke apart. It is seen from figure 19 that the force increased linearly right up to the break; this condition indicates a brittle failure at the interface between the samples.

Measurement of Sputtering and Contamination Rates

Since the total pressure during the ion bombardment was about 8×10^{-6} torr, it was important to know the partial pressure of the gases in the vacuum chamber because if a significant amount of these gases would adsorb on the sample surfaces, these surfaces could have been contaminated faster than they were being cleaned.

In order to determine the effectiveness of the sputtering process, the ratio of the number of nickel atoms sputtered per second to the maximum number of molecules that could have adsorbed per second was calculated. If this ratio, which will be called ζ , was large, the nickel was being removed from the surface much faster than the surface was being recontaminated. The ratio ζ was calculated from

$$\zeta = \frac{S}{F} \quad (3)$$

where S is the sputtering rate given by

$$S = I_+ Y \quad (4)$$

where I_+ is the number of ions per centimeter² per second that impinge on the sample face and is calculated from the ion current, and Y is the sputtering yield in atoms of nickel removed per incident argon ion (ref. 19).

The maximum contamination rate was calculated by assuming all the molecules except argon that struck the sample area adhered to it. This condition is admittedly not true, since the sticking probability for all the gases on nickel is not unity, but the assumption of a unity sticking coefficient gives the maximum possible contamination.

The flux of molecules striking the sample can be calculated from

$$F = \sum F_i = \sum \frac{p_i}{(2\pi m_i k T_i)^{1/2}}$$

or, alternately,

$$F_i = 3.513 \times 10^{22} \frac{p_i}{(M_i T_i)^{1/2}} \quad (5)$$

where p_i is the partial pressure of the i th gas in torrs, M_i is the molecular weight of the i th gas, and T_i is the temperature of the i th gas. The partial pressure of each of the gases present in the vacuum system during the ion bombardment was measured with the mass spectrometer. The value of the ratio ζ varied from 200 to 1000 during the course of the experiment. This value was considered to be sufficient to prevent any recontamination of the sample surfaces while they were being sputtered.

RESULTS AND DISCUSSION

Discussion of Work Function Measurements

As discussed previously, the method used to clean the surfaces of the samples was the ion-bombardment-heating technique. It has been shown that if enough cycles of ion bombardment and heating are employed, single crystals of nickel can be cleaned, and the

diffraction patterns of a clean surface can be obtained in a LEED device (ref. 5). Since in this experiment no such device was possible, the question arose as to the number of cleaning cycles required to clean the samples in this experiment. The answer to this question came from the measurement of the change in work function of the surface.

Change of Work Function With Ion Bombardment

As previously discussed, the work function of a metal is changed when gases are sorbed on the surface. If some contaminant gas such as oxygen is on the surface and that surface is ion bombarded, some of the oxide layer will be sputtered away. If the work function is measured before and after the ion bombardment, the work function will be changed because some of the oxide has been removed. The work function should continue to change with additional ion bombardment until the oxide layer is removed. This simplistic picture must be modified somewhat because the ion-bombardment process is causing argon ions to be "buried" in the surface of the metal, and because there is some diffusion of contaminants from the bulk of the metal to recontaminate the surface.

The first test was to measure the change in work function during ion bombardment. This test was conducted to determine how much ion bombardment was necessary in each cleaning cycle. The specimen had been initially degassed for 2 hours at 550° C before the ion bombardment procedure began. The sample was bombarded until the dosage was 10^{-4} coulomb (the sample area was 0.73 cm²) and then the work function was measured. The ion bombardment was then resumed, and the work function was measured at increments of approximately 10^{-4} coulomb. The results of this procedure are shown in figure 20. The relative work function, which is the work function measured from some fixed arbitrary voltage, decreased steadily from 0.24 eV at 10^{-4} coulomb to -0.06 eV at approximately 32×10^{-4} coulomb. At 32×10^{-4} coulomb, the work function no longer changes as the dosage is increased. Subsequent tests repeating this procedure showed that if the samples were heated to 550° C prior to the ion bombardment, the results shown in figure 20 could be repeated with the same results at approximately 32×10^{-4} coulomb. The fact that the work function was no longer changing with dosage after 32×10^{-4} coulomb was interpreted as meaning that the sputtering process had removed as much of the surface contamination as it was going to remove in that particular cycle of ion bombardment. In the ion bombardment part of the cleaning cycle, the dosage for each ion bombardment was then set at 32×10^{-4} coulomb. (When the sample area is taken into account, the dosage was 44×10^{-4} coulomb per square centimeter.)

Brock (ref. 18) measured the change in the work function with ion bombardment for tungsten and stainless steel. For each of these metals the work function decreased with increasing dosage until at some dosage the work function no longer decreased. This dosage was 1×10^{-4} coulomb per square centimeter for the tungsten and 5×10^{-4} coulomb per square centimeter for the stainless steel.

Change of Work Function With Cleaning Cycles

With the ion bombardment dosage for each cycle determined, the next question was the number of these cycles required to clean the samples. This answer was determined by alternately ion bombarding and heating the samples and measuring the relative work function after each ion bombardment and each heat step. The results of these measurements are shown in figure 21. Only the measurements after heating are presented in the figure because the surface after heating is in the cleanest state. The relative work function increased from -0.09 eV after the first heating cycle to 0.75 eV after the fourth heating cycle to 0.76 eV after the fifth heating cycle. The relative work function changed only slightly between the fourth and fifth cleaning cycles and seems to have stopped varying with the cleaning cycles after about the fifth cycle. The invariance of the work function with further cleaning indicates that the surface is then as clean as the ion-bombardment-heating cleaning process is going to get it. The surface was thus considered to be in its cleanest state for the purposes of this investigation after the fifth cleaning cycle. Some confidence that the ion-bombardment-heating cleaning technique will indeed produce clean surfaces and that the surface after the fifth cleaning cycle is relatively free from contamination is given by the work of Farnsworth and his coworkers. (See ref. 5.)

ADHESION MEASUREMENTS

Effect of Cleaning Cycles

Since the number of cleaning cycles required to clean the surface had been determined, the next tests were conducted to determine the number of cleaning cycles required to get the maximum amount of adhesion. The samples were bombarded and heated for one cleaning cycle, and the sample surfaces were joined with 150 pounds of contact force. The contact force was maintained for 5 minutes, and then the samples were pulled apart and the force required to break the adhesion couple was measured.

The samples were then cleaned and the breaking force measured until the maximum breaking force was attained. Each cleaning cycle consisted of the same ion dosages and temperatures as was used to generate the data in figure 21. The results of a series of these tests are shown in figure 22. The breaking force F_b is divided by the maximum breaking force $F_{b,max}$ attained in that particular test. The breaking force generally increased with increasing number of cleaning cycles to a maximum after the fifth cycle and then does not increase with additional cleaning cycles. The breaking force then increased as the surface was cleaned and attained its maximum value at the same number of cleaning cycles as was required to obtain the cleanest surface. There is some variation between the rates of increase shown in the three tests in figure 22. This difference is attributed to the variation between tests of other parameters such as the hardness.

The characterization of the degree of cleanliness of the surface by using the change in the work function gives a quantitative measure of the number of cleaning cycles required to attain the maximum adhesion force.

It was found that both the ion bombardment and heating parts of the cycle were necessary to get any adhesion of the test samples. A test was conducted in which 400 pounds (1779.2 N) of contact force was used after the samples had been heated at 550° C for 2 hours. No adhesion was measured. Another test was conducted in which the samples were ion bombarded for a dosage of 10^{-1} coulomb per square centimeter and then put together with 200 pounds (889.6 N) of contact force. Again no adhesion occurred.

Oxygen Recontamination

If the sample surfaces are recontaminated with oxygen, then the adhesion coefficient, which is the breaking force divided by the contact force, should decrease to zero. Figure 23 shows the results of a test series in which the sample surfaces were cleaned and then exposed to oxygen for a specified time and at a specified pressure. After the adhesion coefficient had been measured, the surface was recleaned and exposed to a higher dosage of oxygen. The results of the test show that the adhesion coefficient decreased even for relatively low exposures of 0.23×10^{-6} torr-second. The adhesion coefficient did not become zero, however, until the exposure was 10^{-4} torr-second. If the sticking coefficient for oxygen on nickel is assumed to be one for coverages up to one monolayer, then at least for single monolayer coverage, the exposure is directly proportional to the monolayer coverage. The degree of monolayer coverage is also shown in figure 23 by using the exposure of 2.22×10^{-6} torr-second for one monolayer of oxygen (ref. 20).

Gilbreath and Sumsion (ref. 1) measured the adhesion coefficient of clean, fractured aluminum surfaces as a function of the exposure to oxygen and reported that at an exposure of about 2×10^{-4} torr-second, the adhesion coefficient decreased to zero.

CONCLUSIONS

A method for characterizing the surface cleanliness of a nickel surface during adhesion experiments was studied. The method used the change in work function of the surface as a measure of the surface cleanliness. An analysis of the results of this study has led to the following conclusions:

1. The ion-bombardment and heating cleaning technique can be used to clean nickel surfaces for adhesion studies.
2. The change in the work function of a nickel surface can be used to indicate the surface cleanliness required for the maximum adhesion coefficient to occur.

3. Both the ion-bombardment and heating parts of the cleaning cycle are necessary in order to obtain adhesion of nickel at ambient temperatures.

4. Approximately 10^{-4} torr-second of exposure to oxygen is required to contaminate the clean nickel surface to the condition that no adhesion occurs.

Langley Research Center,
National Aeronautics and Space Administration,
Langley Station, Hampton, Va., October 18, 1968,
129-03-13-01-23.

APPENDIX A

THEORY OF ADHESION OF METALS

At the present time there is not a coherent theory that treats the adhesion of real macroscopic surfaces. One of the principal reasons for the lack of a usable model is that the solid surfaces themselves lack definition. Although much work is being currently conducted in this area, there is not now a clear understanding of what a surface is on either a macroscopic or a microscopic scale.

The microscopic or atomistic approach to surfaces is being carried out with such instruments as the low-energy electron diffraction device (LEED), the field emission microscope, the field ion microscope, and the ion microprobe mass spectrometer. These instruments allow the study of individual atoms or layers of atoms at the surface.

The studies of the surfaces on a macroscopic scale are being conducted by ultra-sensitive profilometers, electron microscopes, and the more traditional methods of metallurgy. Although there is no exact theory to treat the adhesion of metals, some of the existing theories do give some insight into the various phenomena involved.

One interpretation of the energy balance at an interface was developed by Dupré (ref. 21) as

$$W_{AB} = \gamma_{AO} + \gamma_{BO} - \gamma_{AB} \quad (A1)$$

where W_{AB} is the work of adhesion between bulk phases A and B; γ_{AO} is the interfacial energy between phase A and vacuum; γ_{BO} , between phase B and vacuum, and γ_{AB} , between phases A and B.

The Dupré equation (eq. (A1)) predicts that if the surface energy of either of the bulk phases is decreased, the work of adhesion should also decrease. Further, Gibbs' adsorption isotherm (ref. 22) predicts the decrease of surface tension (which is part of the surface energy) with increasing surface contamination. Thus the work of adhesion should decrease with increasing surface contamination.

Many investigations have shown that the adhesion coefficient is decreased when surfaces that were relatively clean were exposed to contamination. Gilbreath and Sumsion (ref. 1), for instance, have shown that the adhesion of copper is decreased by increasing surface contamination and that only chemically active species such as oxygen affected the degree of adhesion.

One limitation to the use of equation (A1) is the lack of data on the surface energy of uncontaminated solid surfaces. Very little data are available in the literature on the surface energies of uncontaminated surfaces. This subject has been discussed in some detail in reference 23.

APPENDIX B

WORK FUNCTION RELATIONSHIPS

The relationships to determine the sample work functions are as follows: The anode current-voltage relationship in the retarding field region is:

$$I = CT^2 \exp \left[\frac{-e(\phi_A - V_A)}{kT} \right] \quad (\text{B1})$$

where

- ϕ_A sample work function
- V_A sample cathode voltage
- T cathode temperature
- C constant

The equation

$$I = \frac{V_B - V_A}{R} \quad (\text{B2})$$

must also hold where V_B is the electromotive force and R is the resistance of the source of current for the diode; therefore,

$$\frac{dV_A}{d\phi_A} = \left[1 + \left(\frac{kT}{e} \right) \left(\frac{1}{V_B - V_A} \right) \right]^{-1} \quad (\text{B3})$$

for a constant cathode temperature. Therefore, if $V_B - V_A \gg \frac{kT}{e}$, then

$$\Delta V_A = \Delta \phi_A \quad (\text{B4})$$

For a cathode temperature of 3000°K , $\frac{kT}{e} \approx 0.25$ volt, and since for this experiment, $V_B - V_A \approx 30$ volts, $V_B - V_A \gg \frac{kT}{e}$.

REFERENCES

1. Gilbreath, William P.; and Sumsion, H. T.: Solid-Phase Welding of Metals Under High Vacuum. *J. Spacecraft Rockets*, vol. 3, no. 5, May 1966, pp. 674-679.
2. Johnson, K. I.; and Keller, D. V., Jr.: Factors Affecting the Adhesion of Titanium and Molybdenum Couples. *J. Vacuum Sci. Technol.*, vol. 4, no. 3, May/June 1967, pp. 115-122.
3. Keller, D. V.: Adhesion Between Solid Metals. *Wear*, vol. 6, 1963, pp. 353-365.
4. Hordon, M. J.: Adhesion of Metals in High Vacuum. Adhesion or Cold Welding of Materials in Space Environments, Spec. Tech. Publ. No. 431, Ameri. Soc. Testing Mater., c.1967, pp. 109-127.
5. Farnsworth, H. E.; Schlier, R. E.; George, T. H.; and Burger, R. M.: Application of the Ion Bombardment Cleaning Method to Titanium, Germanium, Silicon, and Nickel as Determined by Low-Energy Electron Diffraction. *J. Appl. Phys.*, vol. 29, no. 8, Aug. 1958, pp. 1150-1161.
6. Dillon, J. A., Jr.; and Farnsworth, H. E.: Work Function of the (100) Face of a Germanium Single Crystal as a Function of Heat Treatment and Ion Bombardment. *Phys. Rev. (Proc. Amer. Phys. Soc.)*, Second ser., vol. 99, no. 5, Sept. 1, 1955, p. 1643.
7. Boggio, J. E.; and Farnsworth, H. E.: Low-Energy Electron Diffraction and Photoelectric Study of (110) Tantalum as a Function of Ion Bombardment and Heat Treatment. *Surface Sci.*, vol. 1, no. 4, Oct. 1964, pp. 399-406.
8. Mac Rae, A. U.: Adsorption of Oxygen on the $\{111\}$, $\{100\}$ and $\{110\}$ Surfaces of Clean Nickel. *Surface Sci.*, vol. 1, no. 4, Oct. 1964, pp. 319-348.
9. Culver, R. V.; and Thompkins, F. C.: Surface Potentials and Adsorption Process on Metals. *Advance in Catalysis and Related Subjects*, Vol. XI, D. D. Eley, P. W. Selwood, and Paul B. Weisz, eds., Acad. Press, Inc., 1959, pp. 67-131.
10. Eberhagen, A.: Die Anderung der Austrittsarbeit von Metallen durch eine Gasadsorption. *Fortschr. Phys.* vol. 8, 1960, pp. 245-295.
11. Nottingham, Wayne B.: Thermonic Emission. *Handbuch d. Physik*, Bd. XXI, Springer-Verlag (Berlin), 1956, pp. 1-175.
12. Eisinger, Joseph: Electrical Properties of Nitrogen Adsorbed on Tungsten. *J. Chem. Phys. (Lett. Ed.)*, vol. 28, no. 1, Jan. 1958, pp. 165-166.
13. Eisinger, Joseph: Adsorption of CO on Tungsten and Its Effect on the Work Function. *J. Chem. Phys. (Lett. Ed.)*, vol. 27, no. 5, Nov. 1957, pp. 1206-1207.

14. Redhead, P. A.: Chemisorption on Metals Under Ultrahigh Vacuum Conditions. Proceedings of the Symposium on Electron and Vacuum Physics – Hungary 1962, Akadémiai Kiadó (Budapest), 1963, pp. 89-100.
15. Macdonald, J. Ross; and Barlow, C. A., Jr.: Work Function Change on Monolayer Adsorption. J. Chem. Phys., vol. 39, no. 2, July 15, 1963, pp. 412-422.
16. Bradford, James M., Jr.: Operating Parameters of the Omegatron Mass Spectrometer in Ultrahigh Vacuum. NASA TN D-3129, 1965.
17. Crowell, C. R.; and Armstrong, R. A.: Temperature Dependence of the Work Function of Silver, Sodium, and Potassium. Phys. Rev., Second ser., vol. 114, no. 6, June 15, 1959, pp. 1500-1506.
18. Brock, F. J.: Surface Cleaning Techniques in Ultrahigh Vacuum. Contract No. NAS 1-2691, Task #5, Nat. Res. Corp.
19. Weijnsfeld, C. H.: Yield, Energy and Angular Distributions of Sputtered Atoms. Philips Res. Rep. Suppl., no. 2, 1967.
20. Santeler, Donald J.; Holkeboer, David H.; Jones, Donald W.; and Pagano, Frank: Vacuum Technology and Space Simulation. NASA SP-105, 1966.
21. Dupré, Athanase: Theorie mechanique de la chaleur. Gauthier-Villars (Paris), 1869, p. 369.
22. Anon.: The Collected Works of J. Willard Gibbs. Vol. I – Thermodynamics. Vol. 1. Yale Univ. Press, 1948.
23. Keller, D. V., Jr.: The Analysis of Metallic Adhesion Data. Adhesion or Cold Welding of Materials in Space Environments, Spec. Tech. Publ. No. 431, Amer. Soc. Testing Mater., c.1967, pp. 181-207.

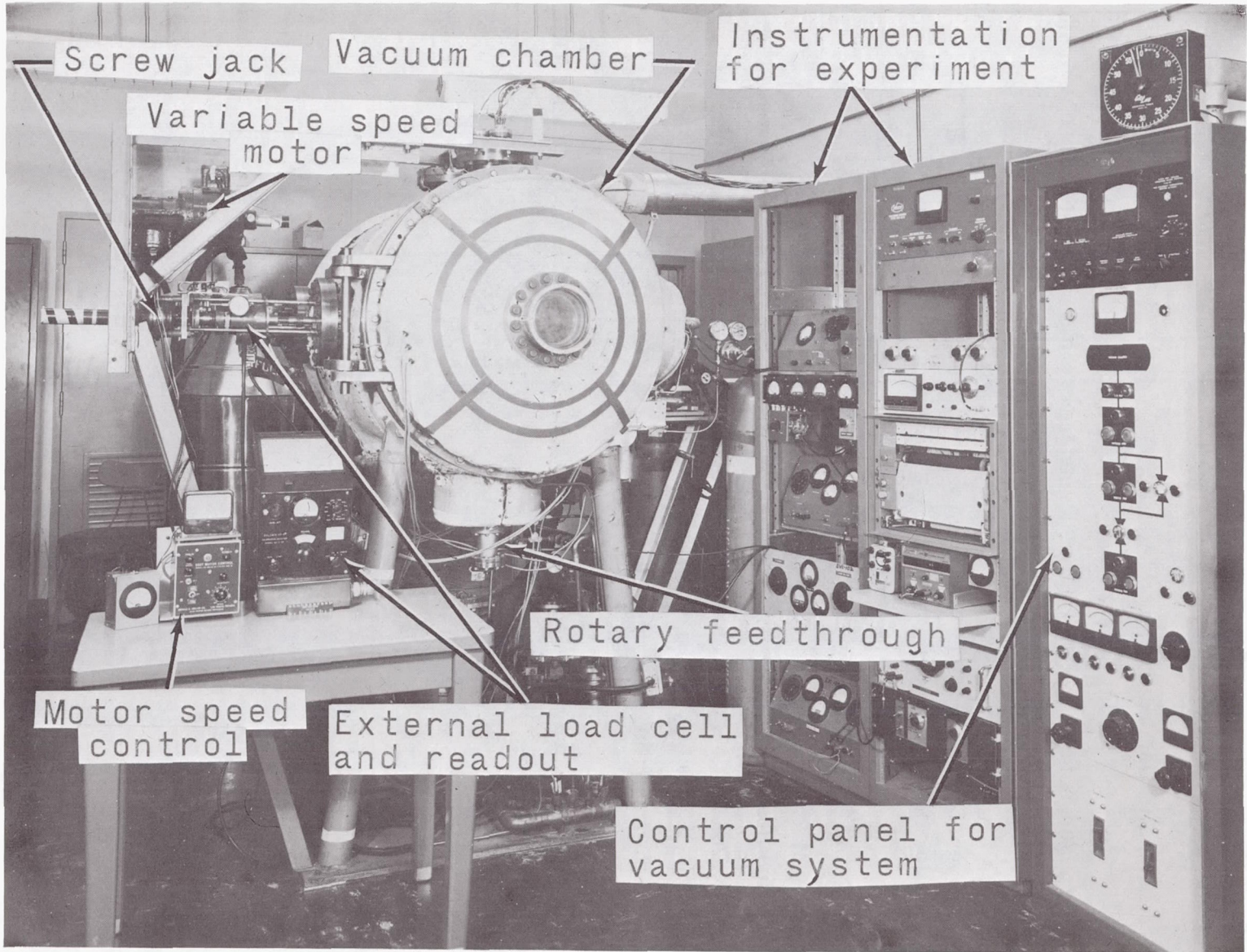


Figure 1.- Vacuum system and instrumentation.

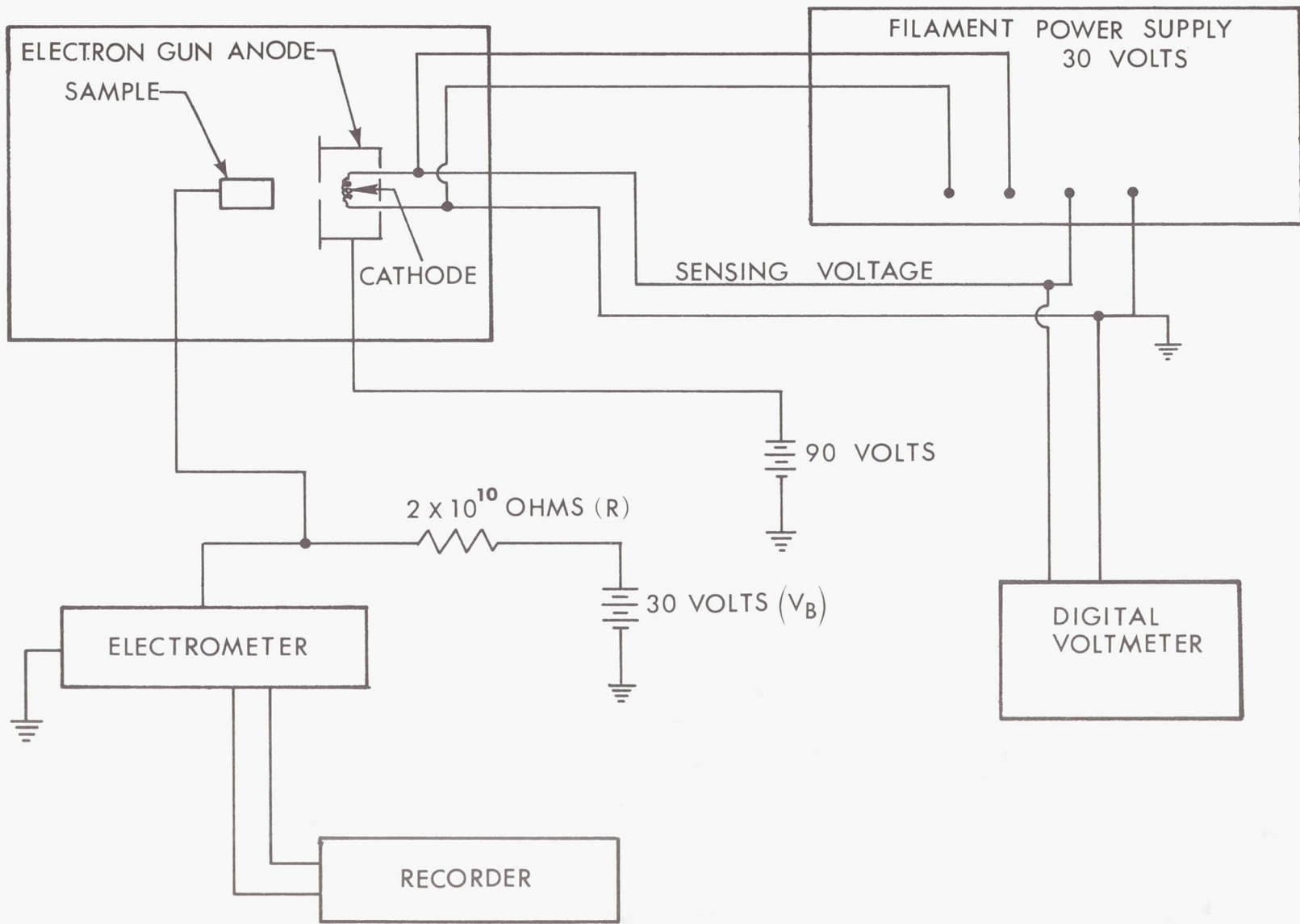


Figure 2.- Electrical schematic of apparatus used to measure work function.

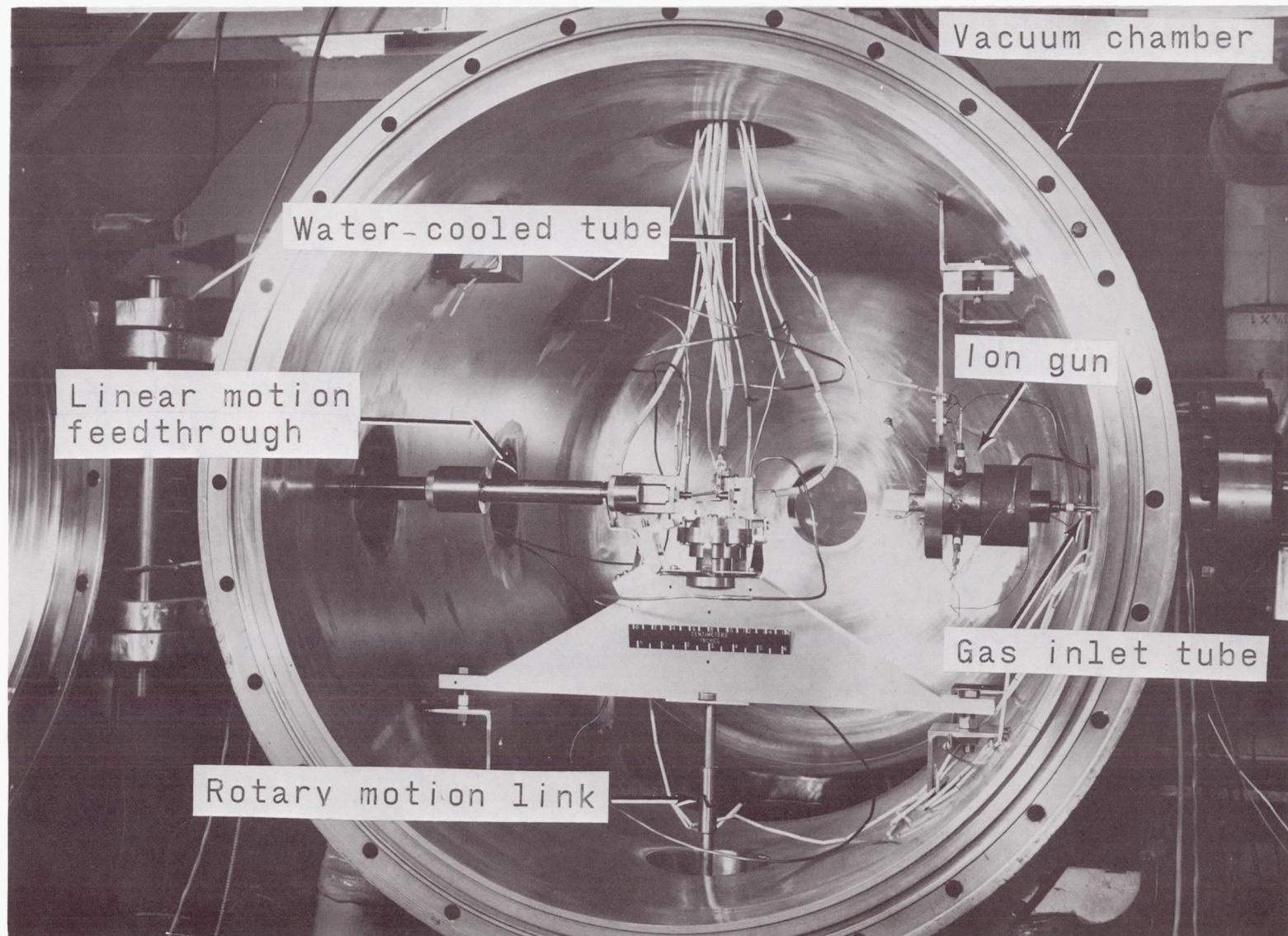


Figure 3.- Apparatus used to measure change in work function.

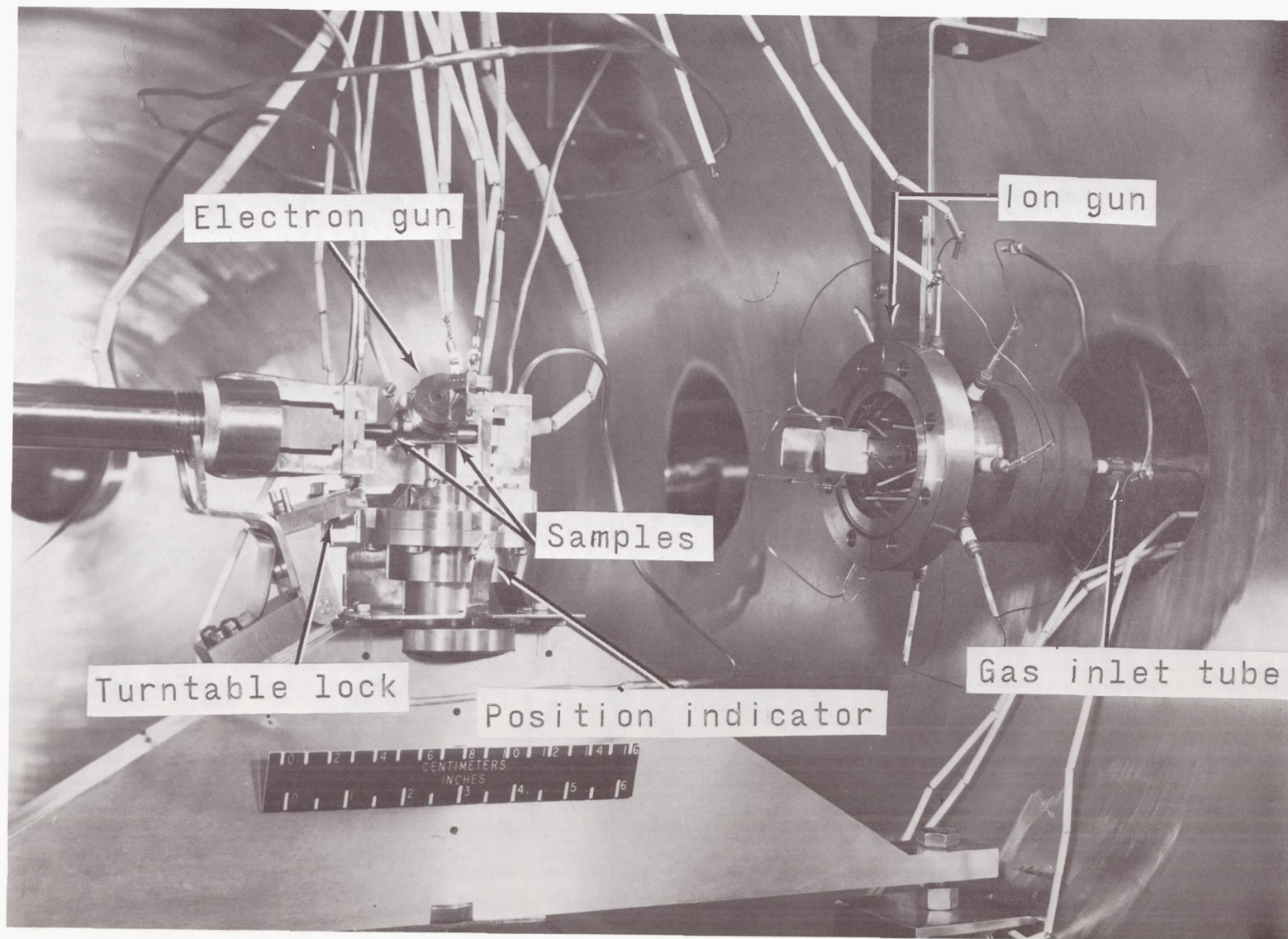


Figure 4.- Closeup of apparatus to measure work function.

L-67-3557.1

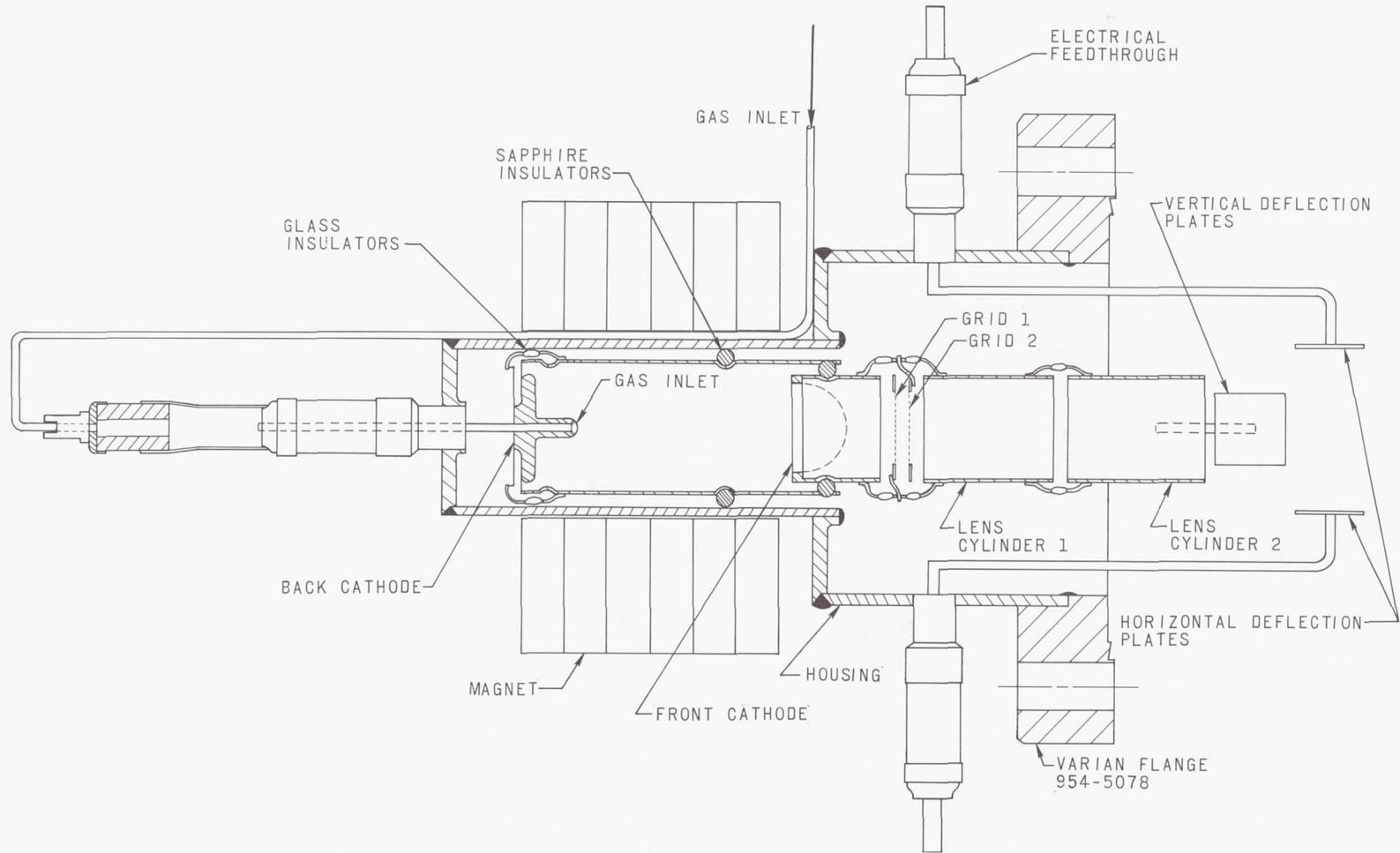


Figure 5.- Magnetron ion gun.

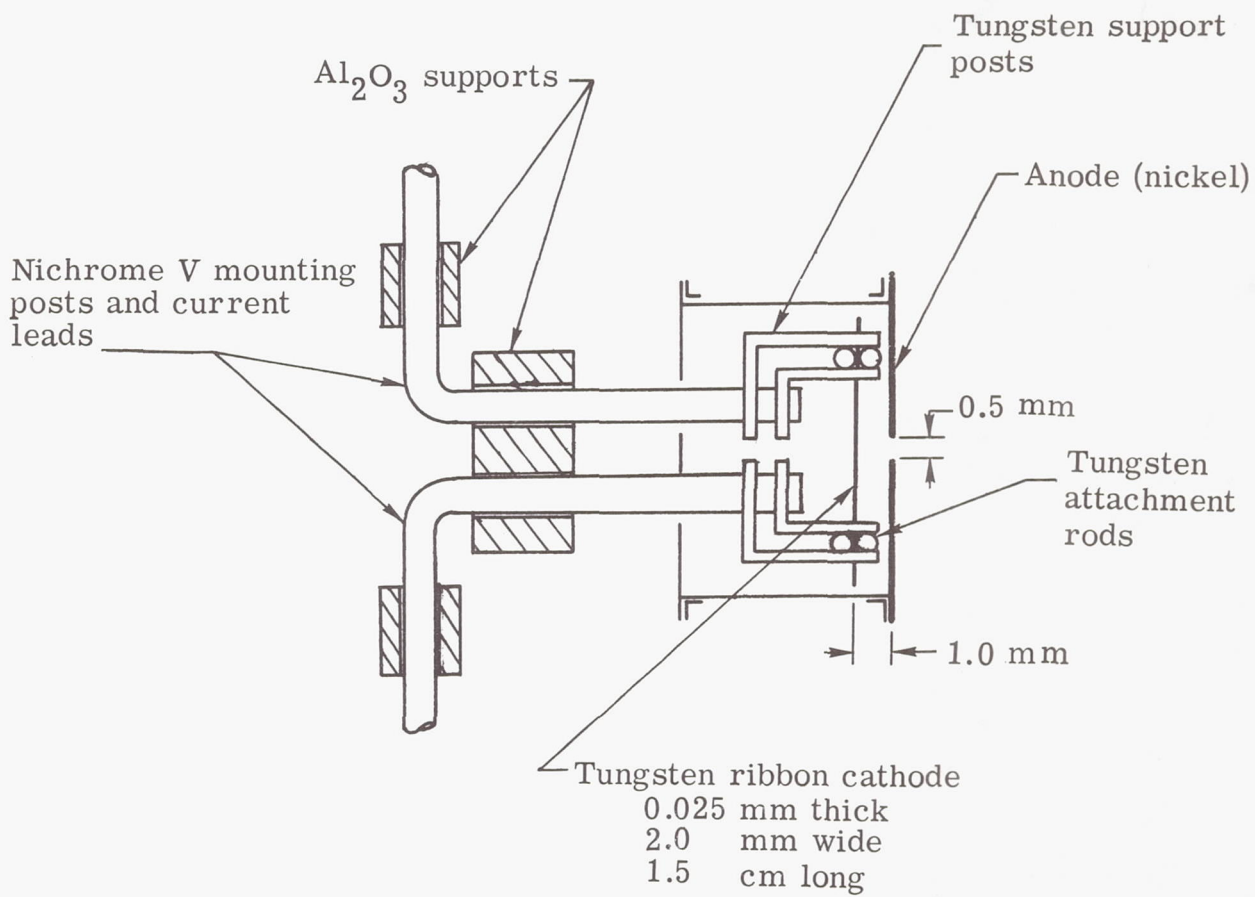


Figure 6.- Electron gun used during work function measurements.

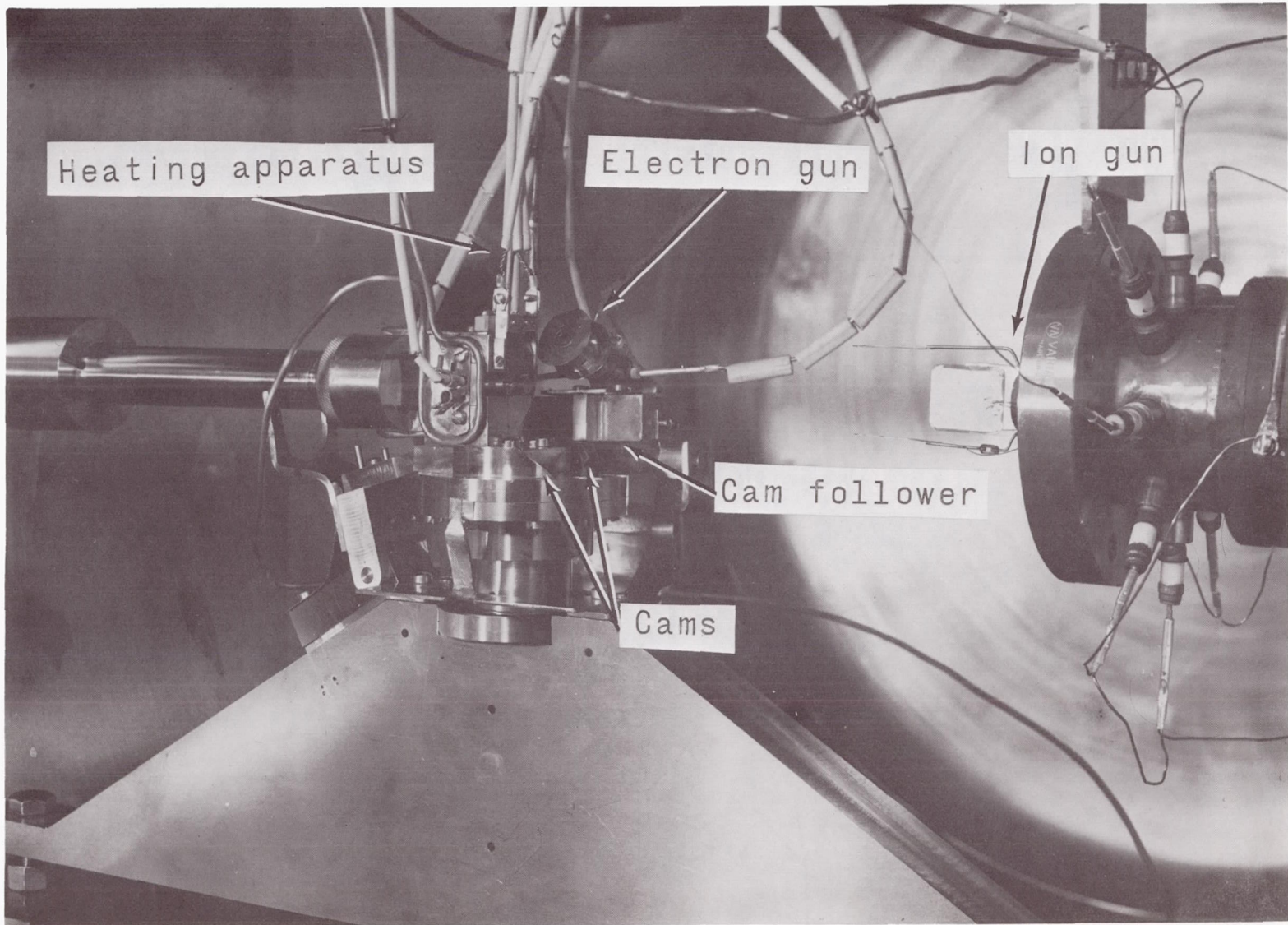


Figure 7.- Rotation apparatus in ion bombarding position.

L-67-3555.1

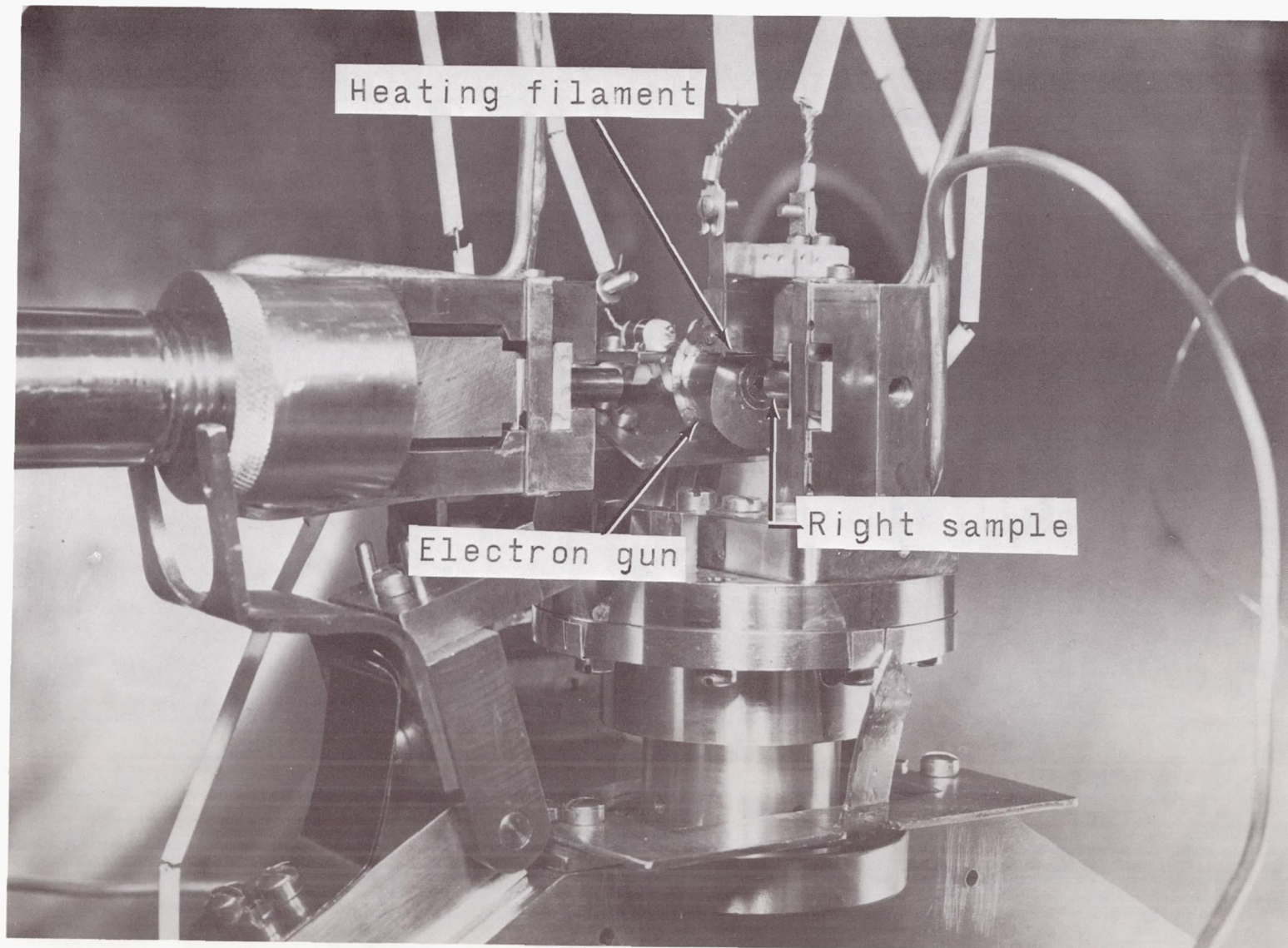


Figure 8.- Rotation apparatus in position to measure relative work function.

L-67-3559.1

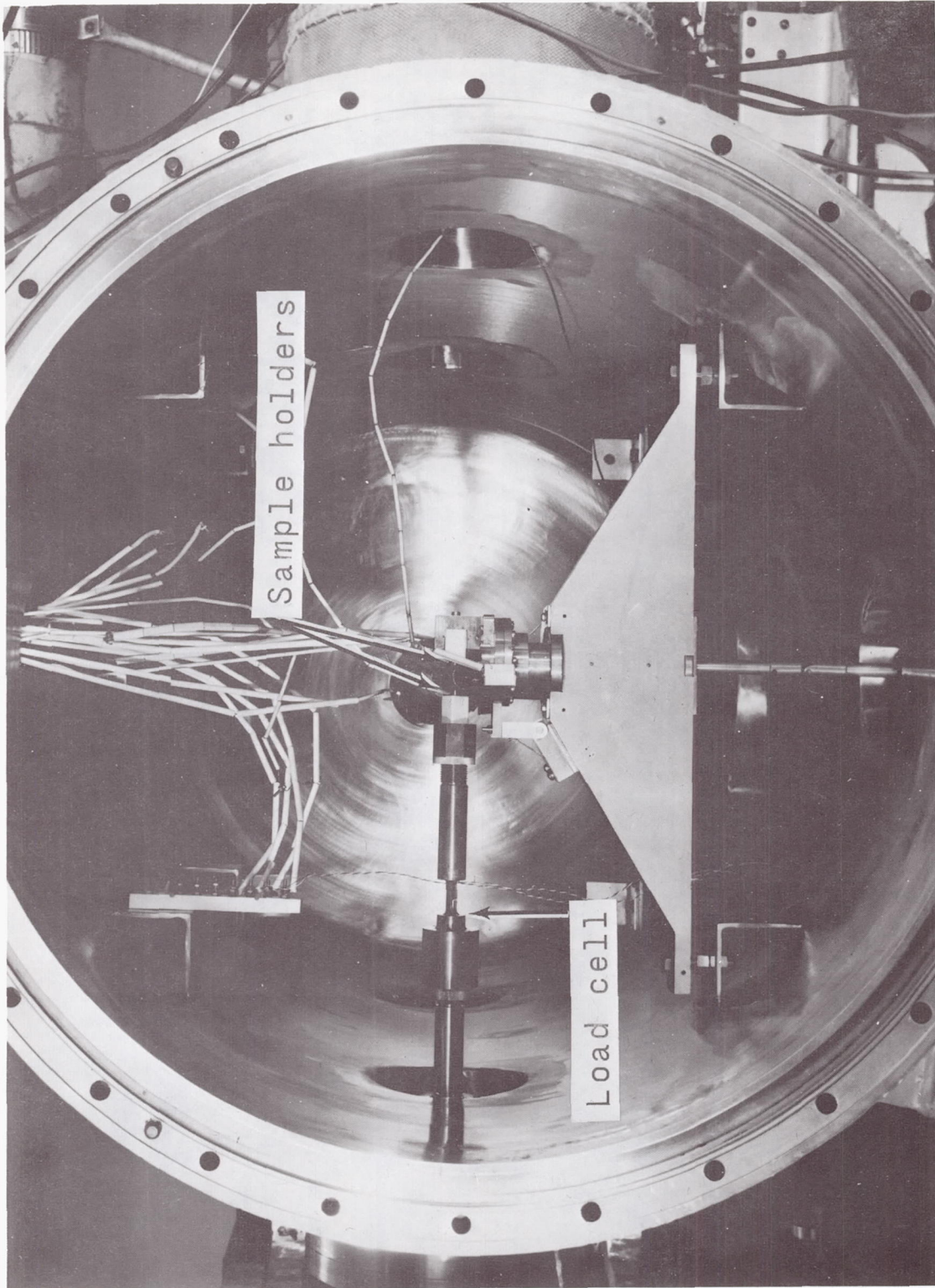


Figure 9.- Adhesion apparatus inside vacuum chamber.

L-68-10,004

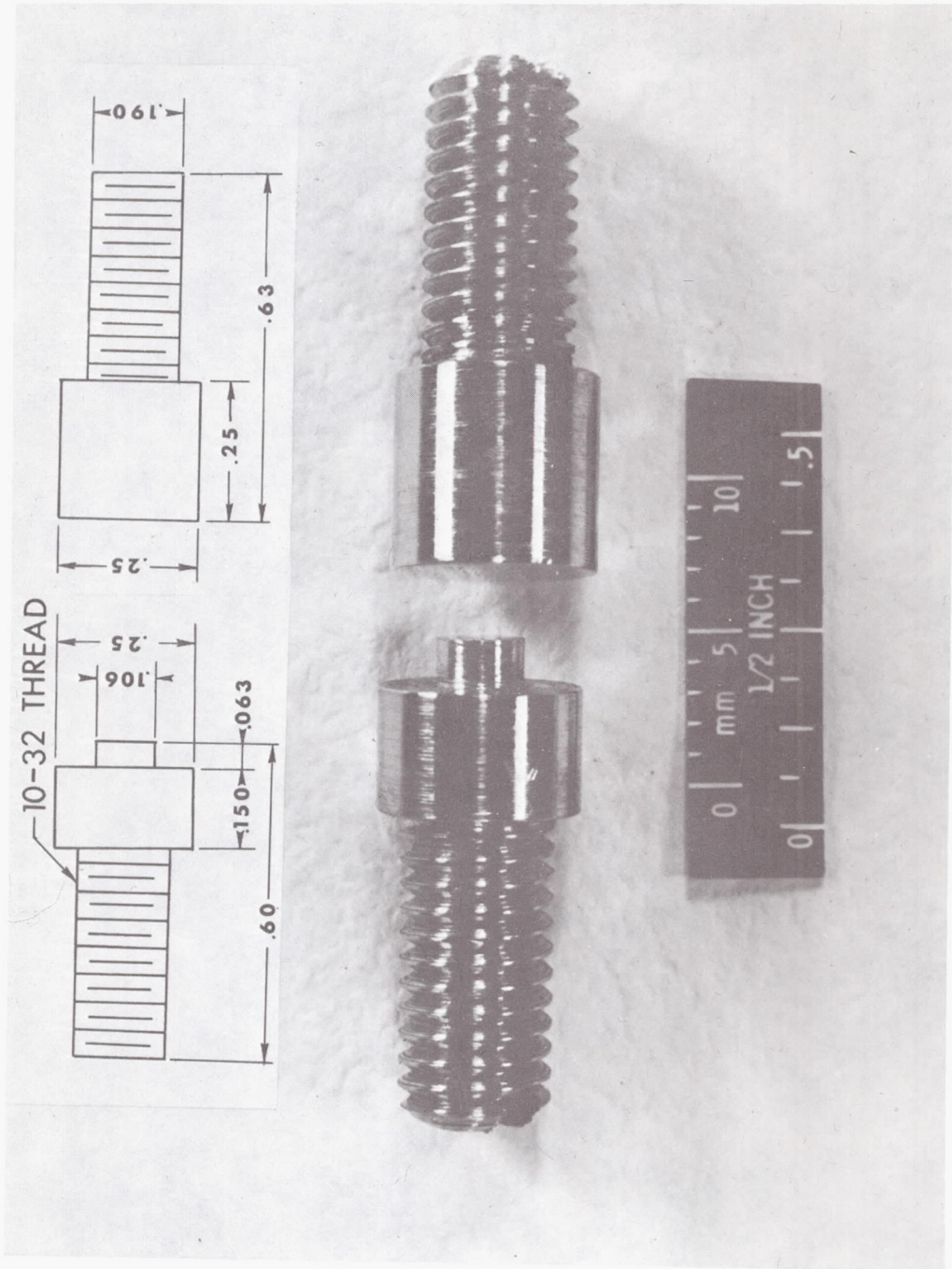


Figure 10.- Set of samples.

L-68-10,005

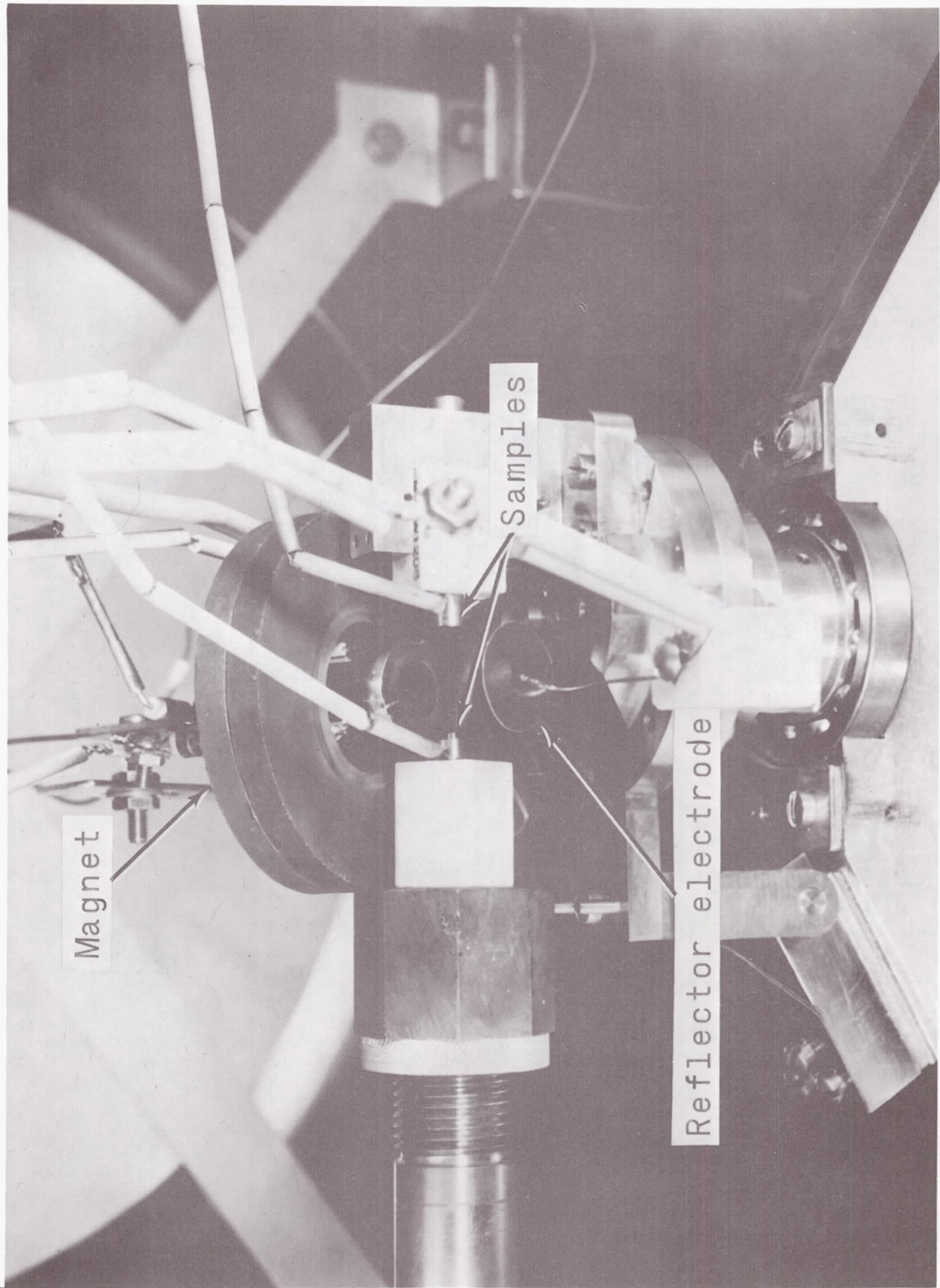


Figure 11.- Closeup of adhesion apparatus.

L-68-10,006

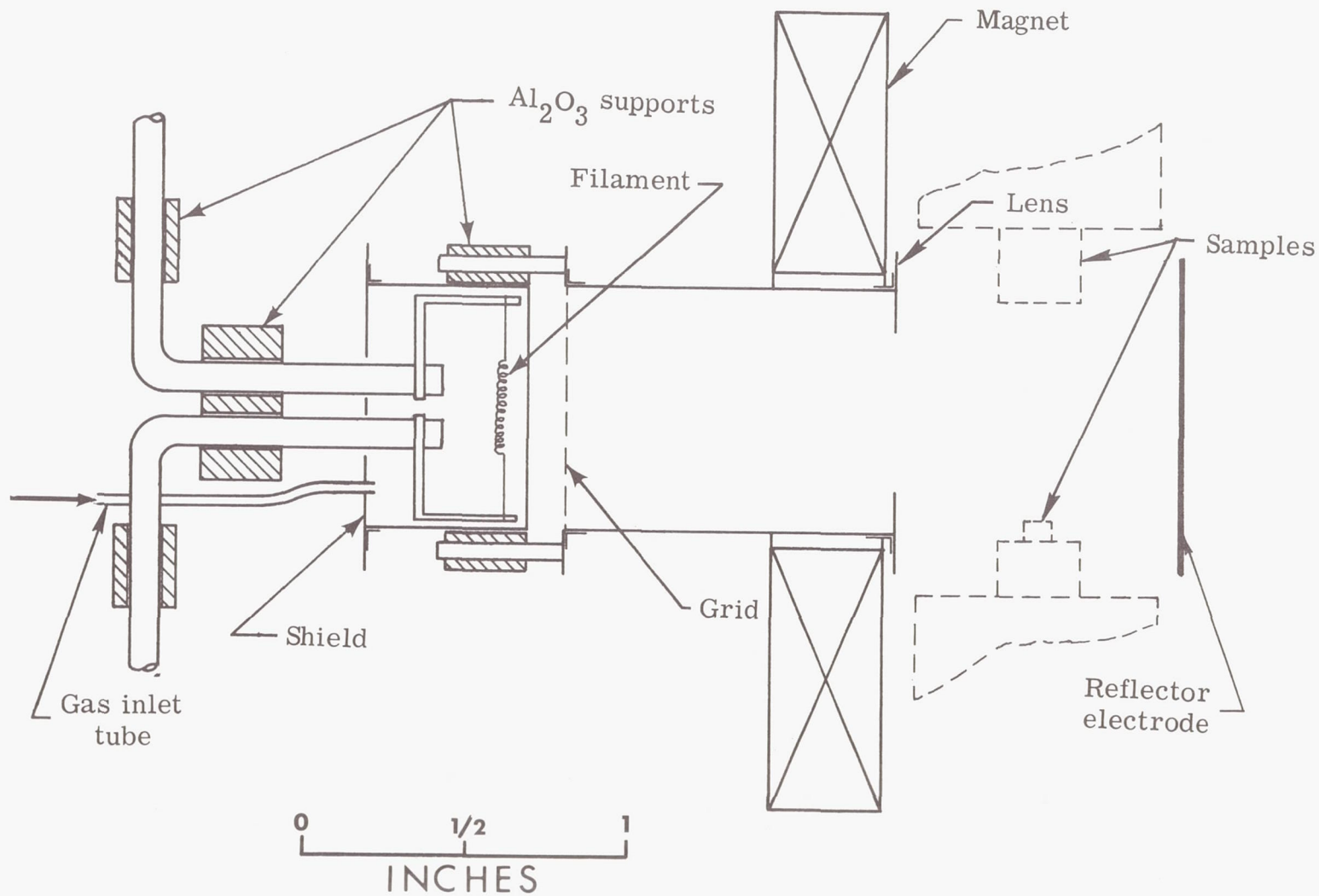


Figure 12.- Hot cathode ion gun.

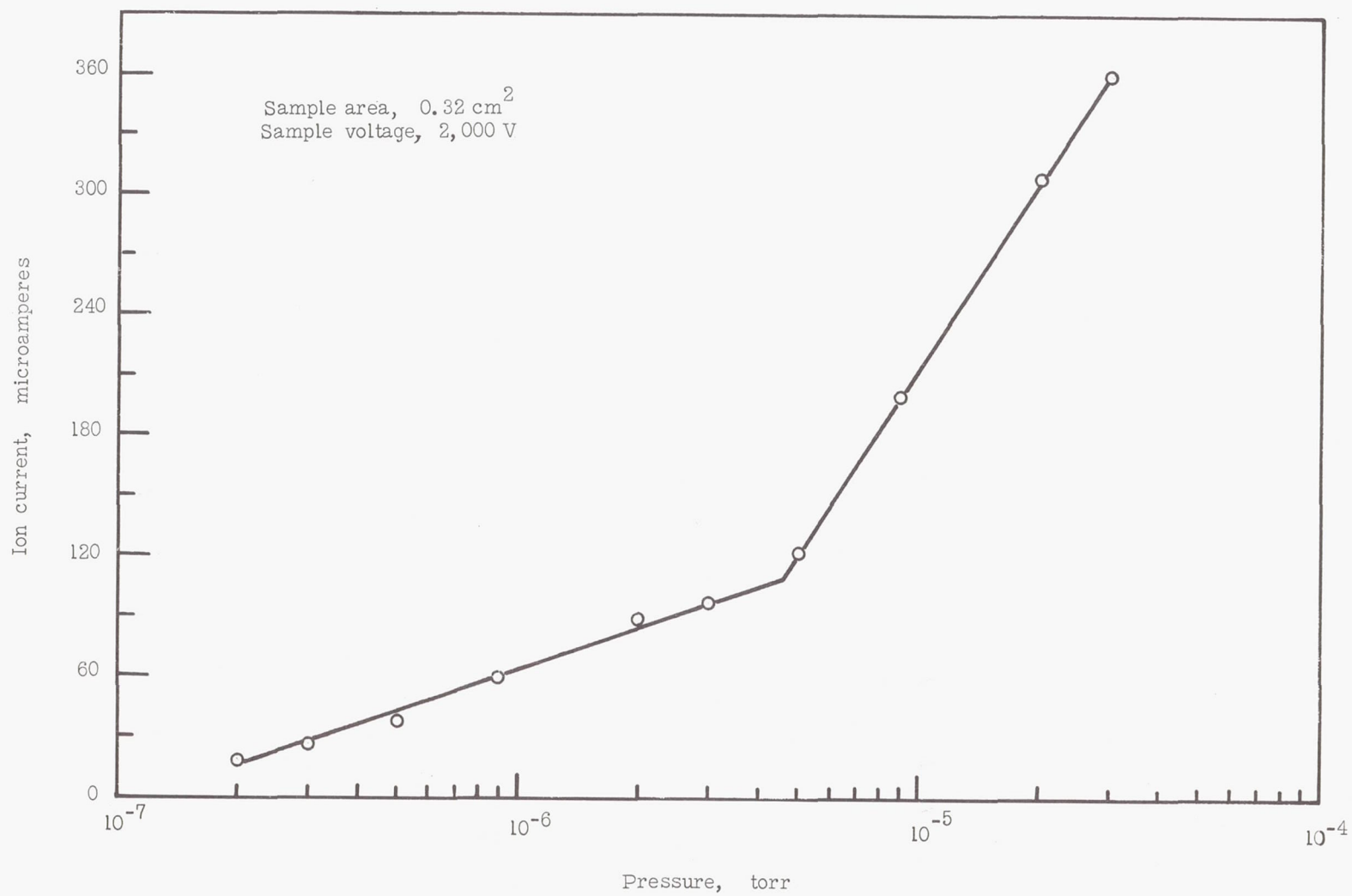


Figure 13.- Variation of ion current with pressure.

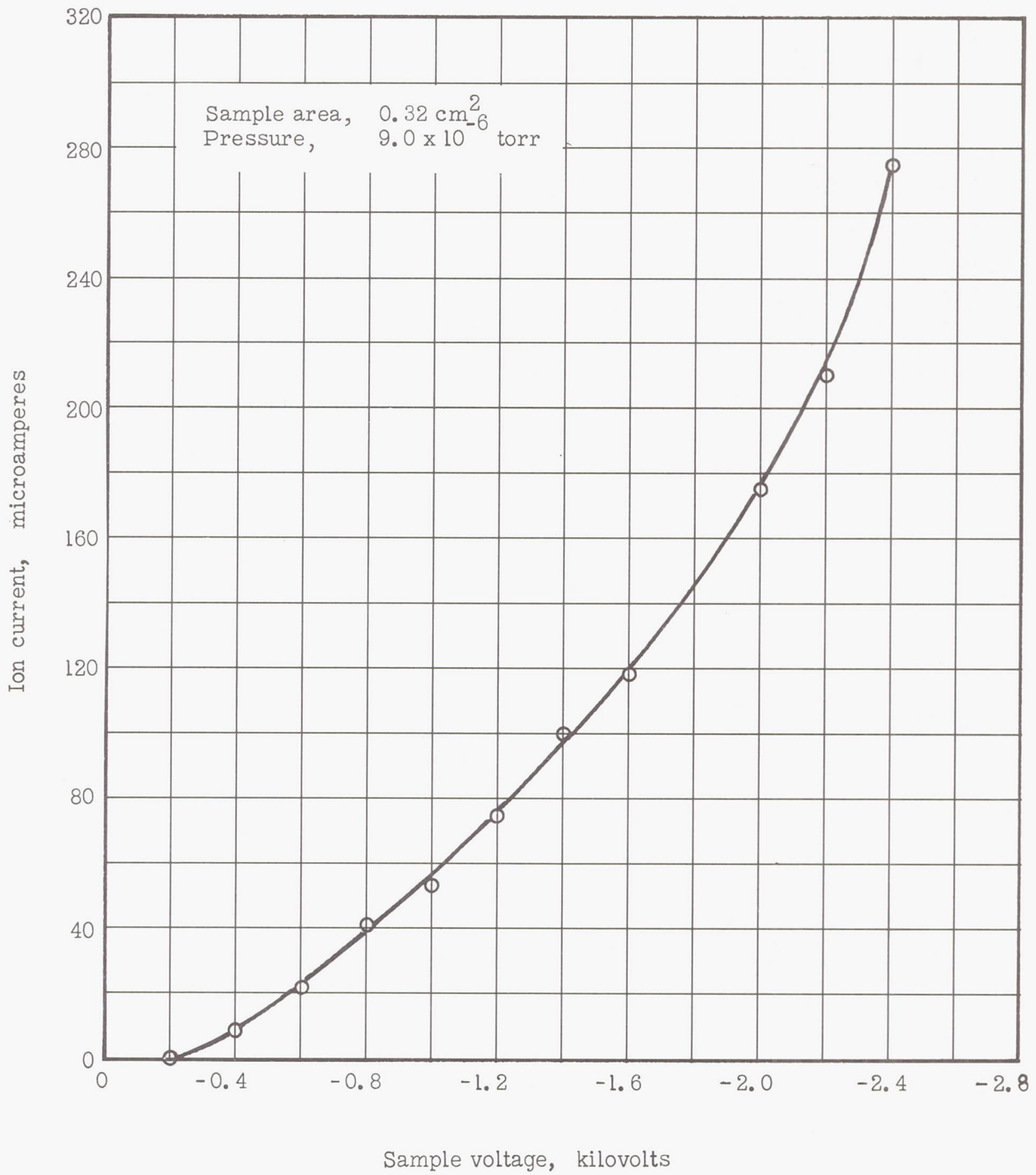


Figure 14.- Variation of ion current with sample voltage.

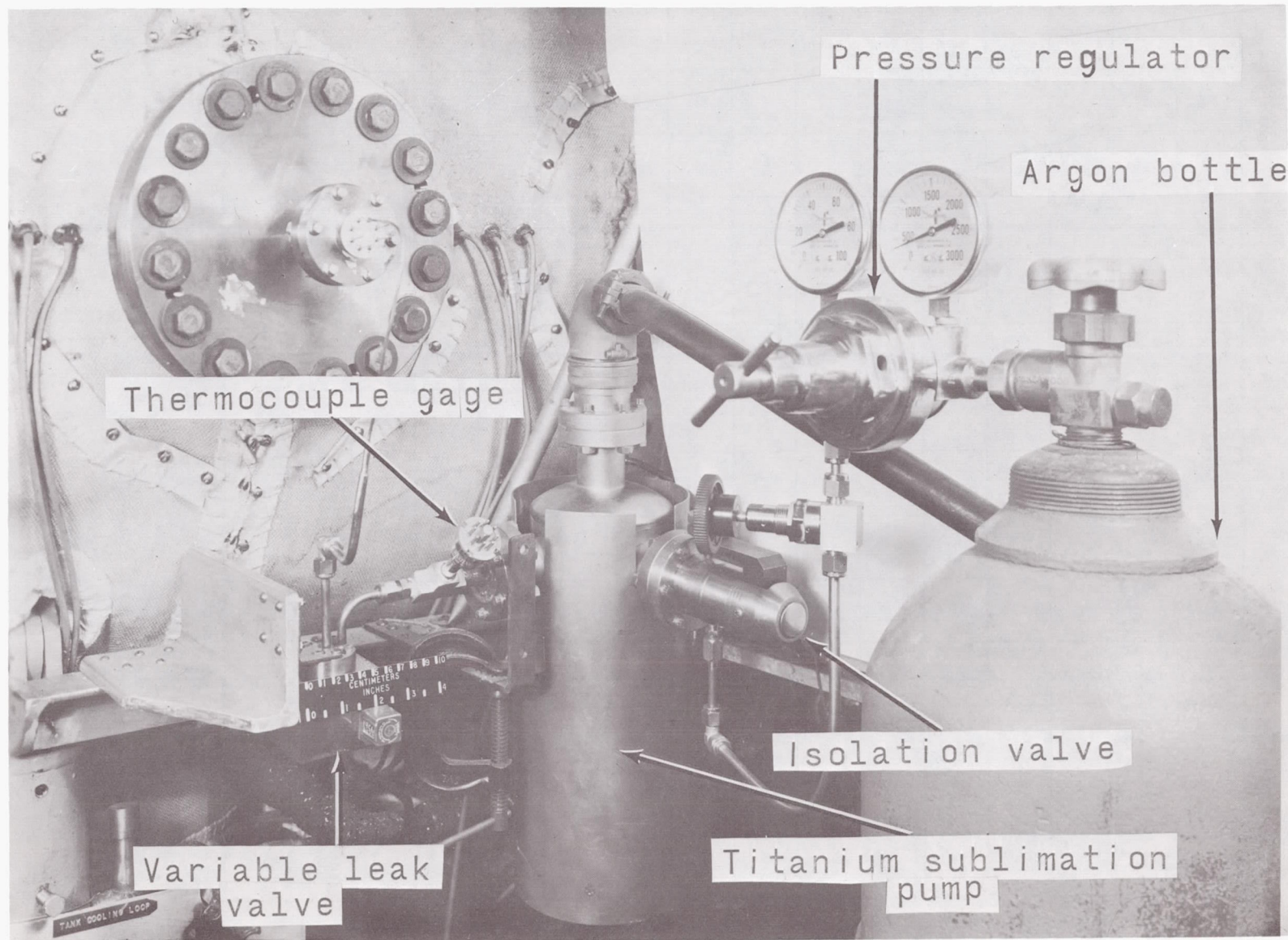


Figure 15.- Gas inlet system.

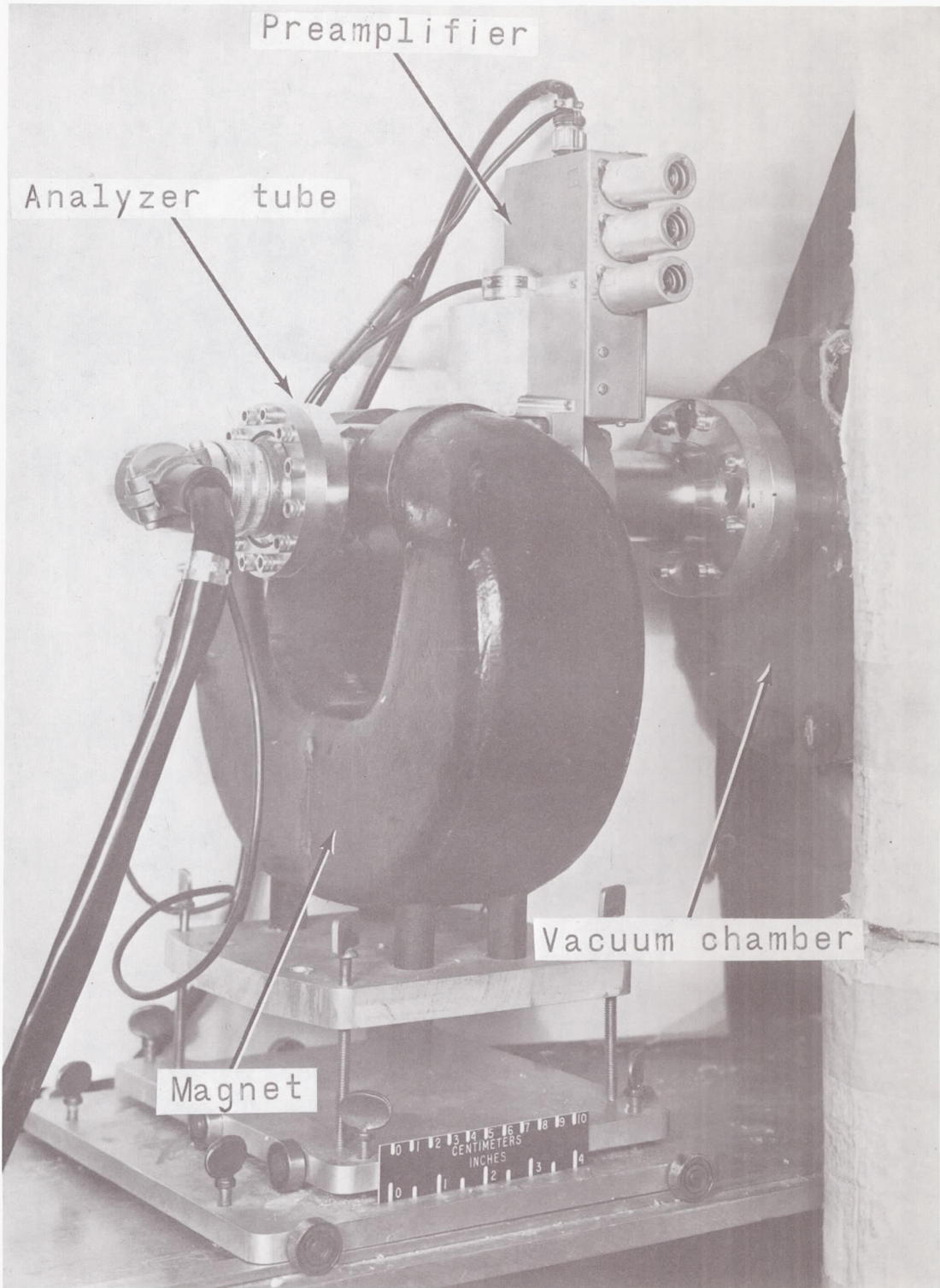


Figure 16.- Mass spectrometer.

L-67-8696.1

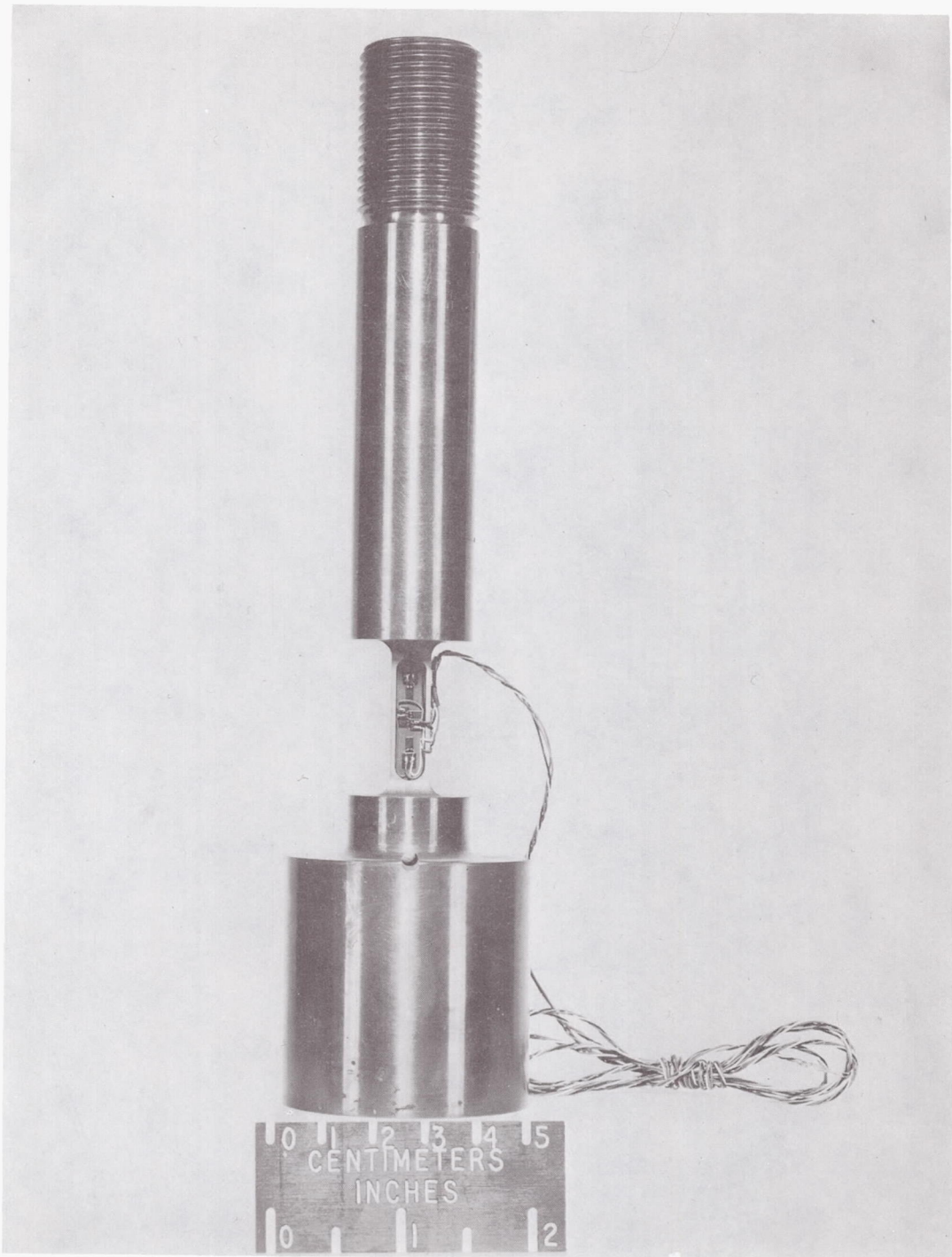


Figure 17.- Closeup of load cell.

L-67-8246

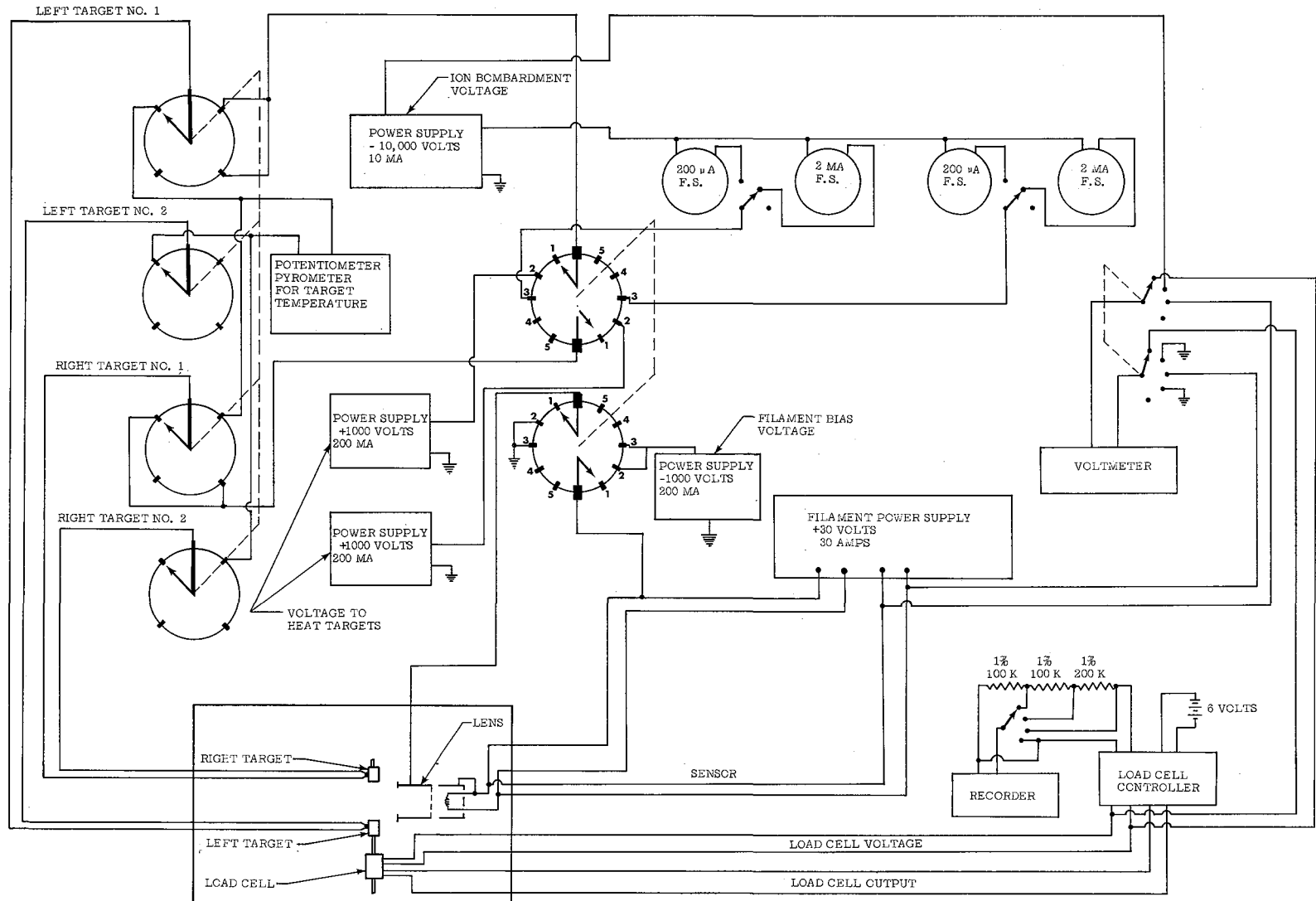


Figure 18.- Electrical circuit for adhesion apparatus.

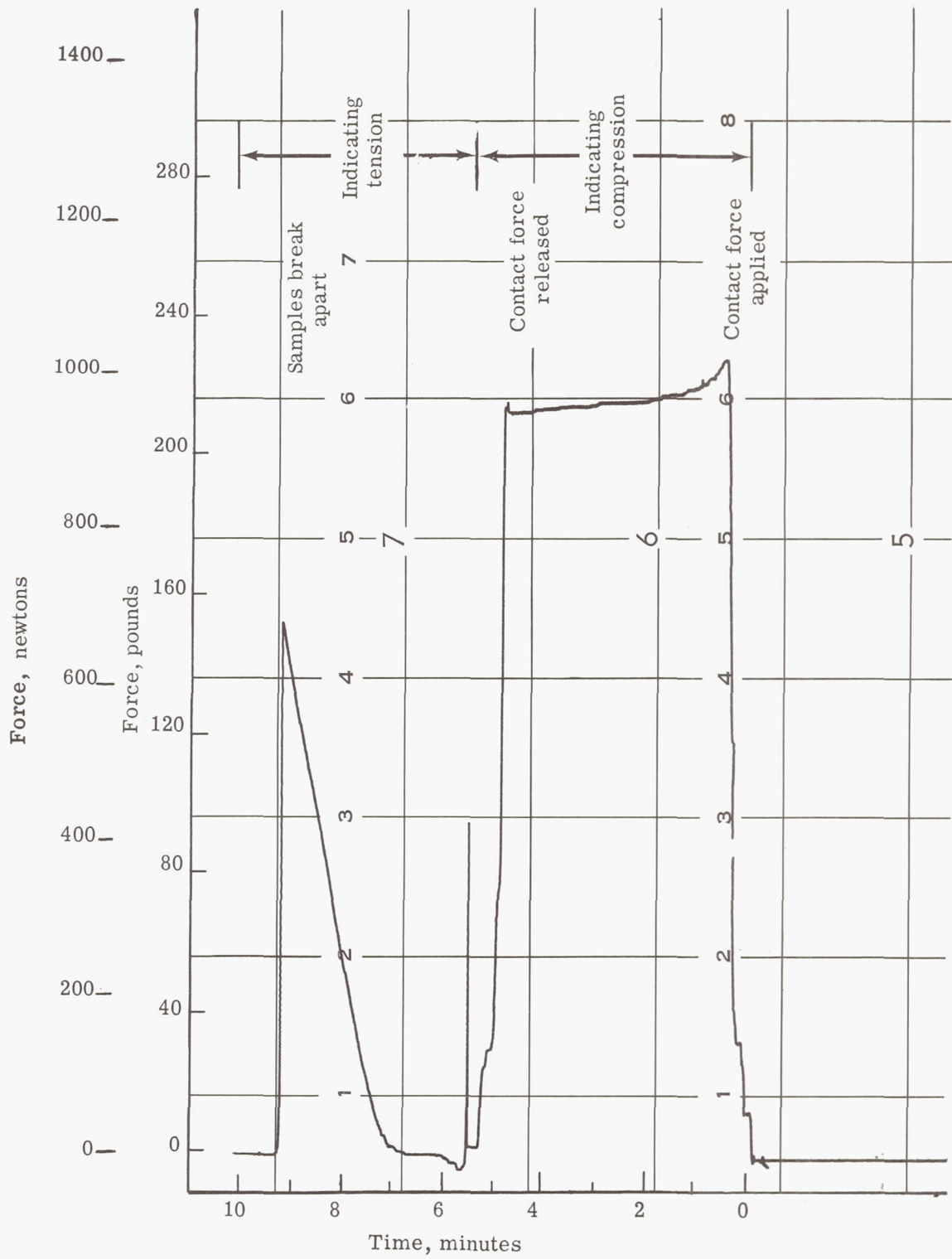


Figure 19.- Example of recorder trace during measurement of adhesion coefficient.

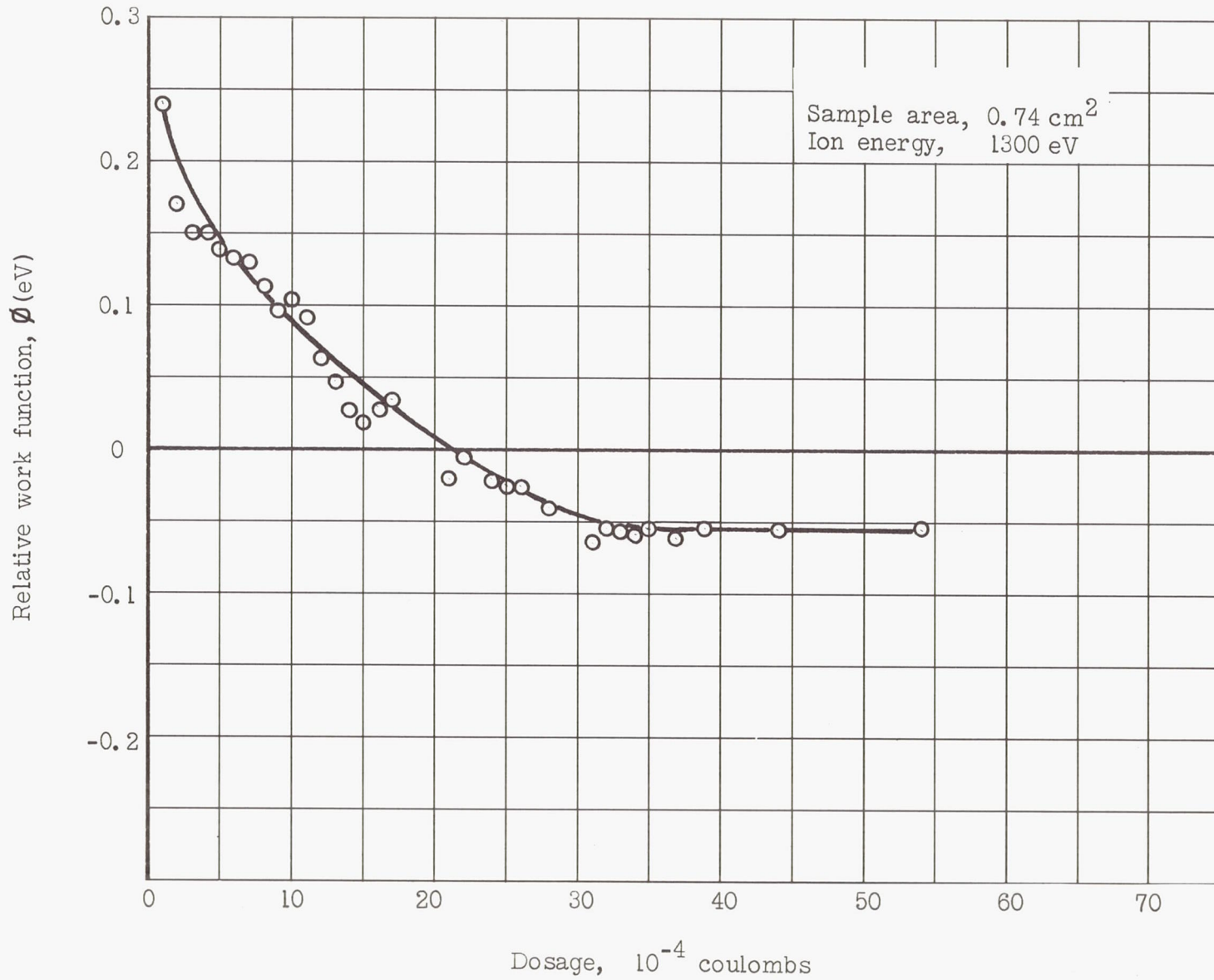


Figure 20.- Variation of relative work function with dosage.

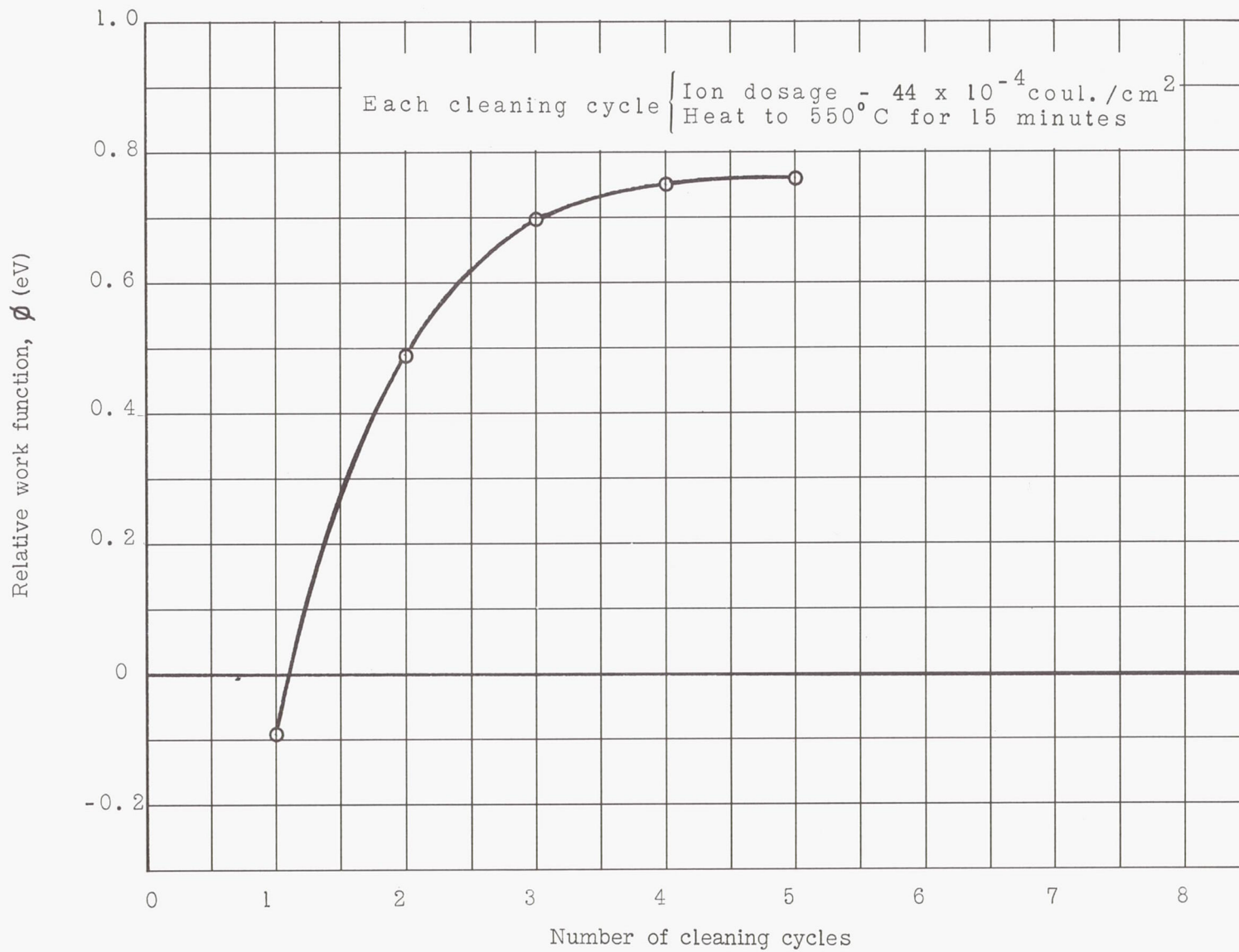


Figure 21.- Variation of relative work function with number of cleaning cycles.

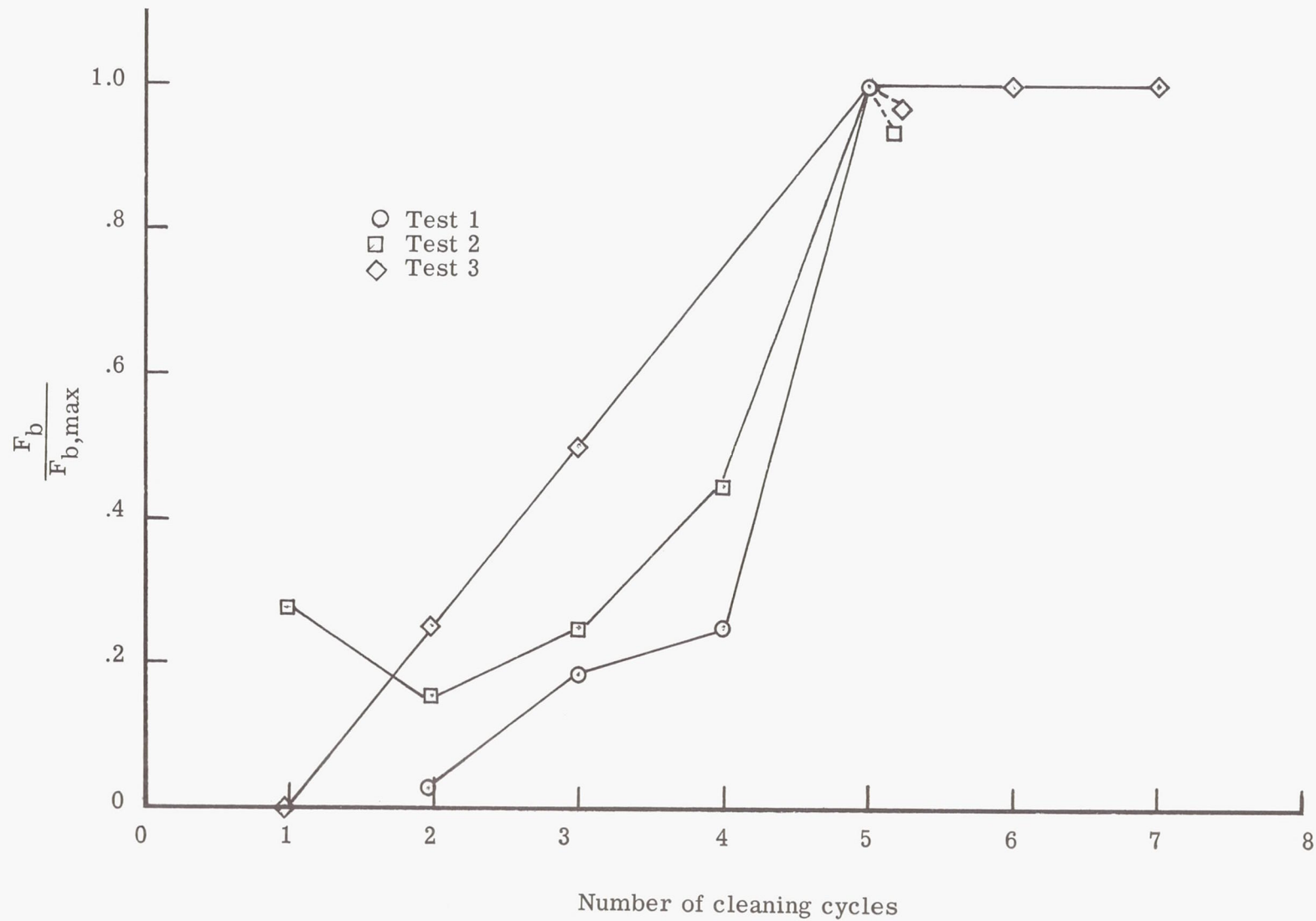


Figure 22.- Variation of adhesion efficiency with number of cleaning cycles.

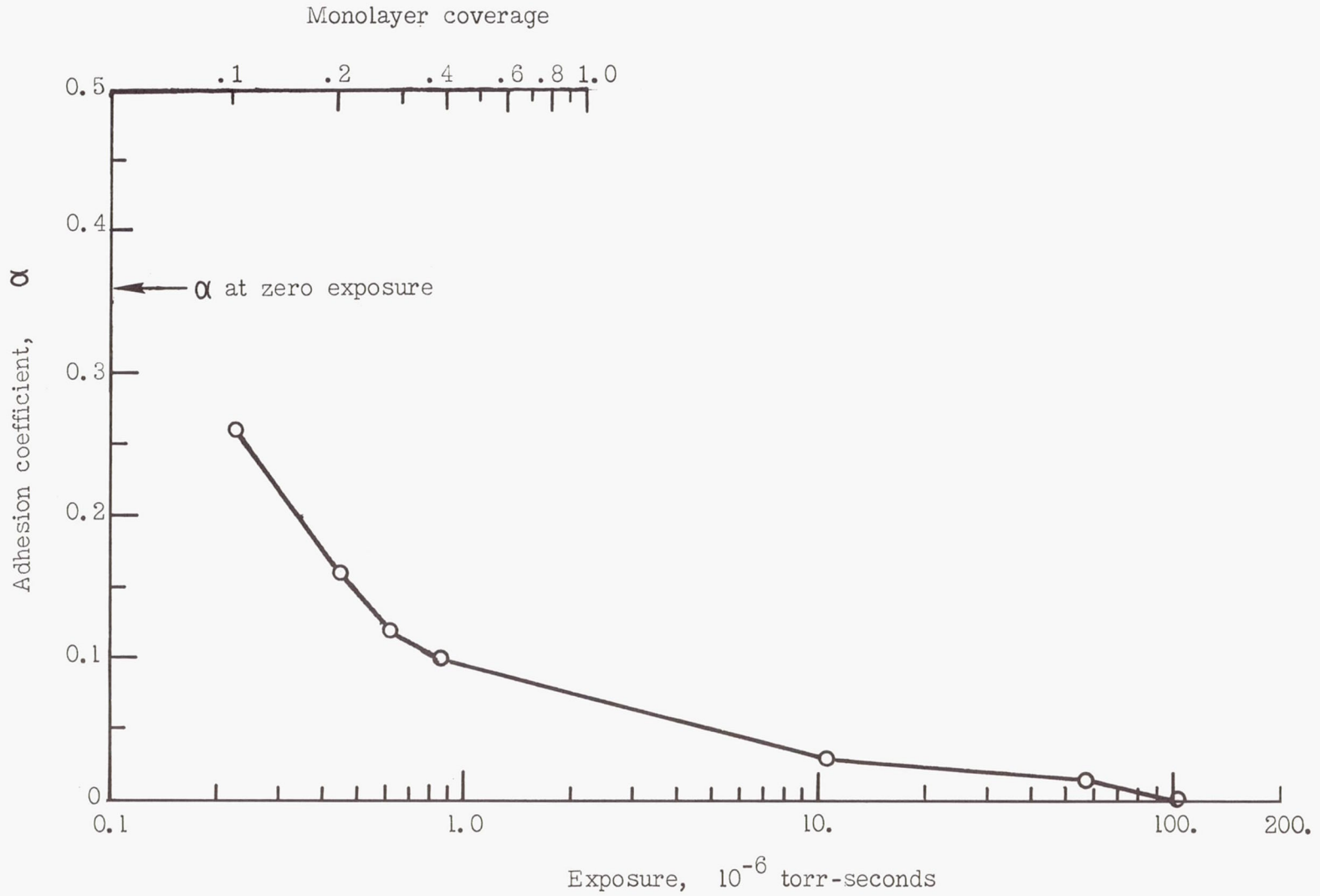


Figure 23.- Variation of adhesion coefficient with oxygen exposure. Contact force, 50 pounds (222.41 newtons).